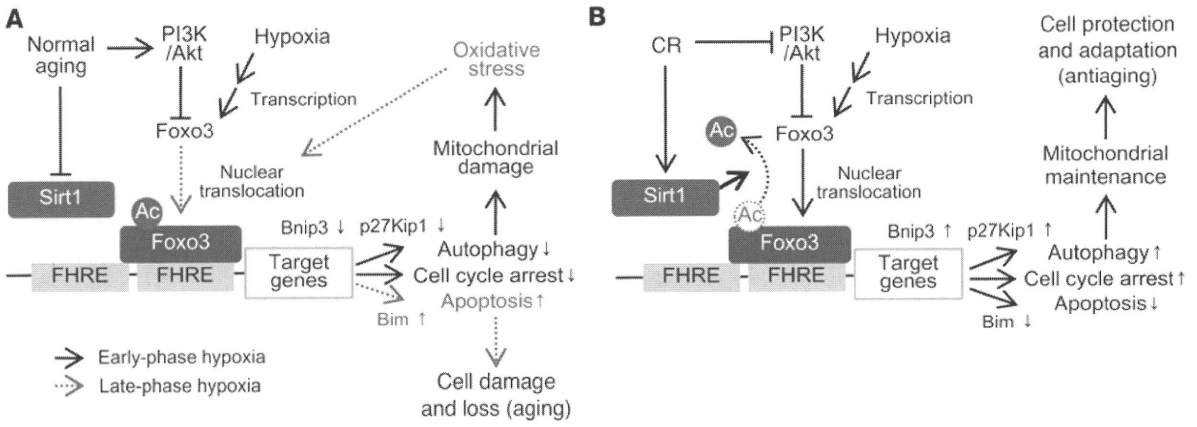


**Figure 10**

Molecular mechanisms underlying CR-mediated cellular adaptation to hypoxia in aged kidney. (**A**) The normal aging process inhibits Sirt1 activity. During early-stage hypoxia, hypoxia fails to enhance nuclear translocation of Foxo3, subsequent autophagy, and cell cycle arrest, which increases mitochondrial oxidative damage (black lines). At late-phase hypoxia, hypoxia-associated oxidative stress activates nuclear translocation of acetylated Foxo3, which promotes apoptosis (red lines). (**B**) CR activates Sirt1 activity and nuclear translocation of Foxo3, which promotes autophagy and cell cycle arrest under hypoxia to maintain normal mitochondria function under hypoxia.

lar mechanism of CR-mediated cell adaptation to age-associated hypoxia. Because stress-induced apoptosis and cell loss have been implicated in age-associated diseases (47), Sirt1 deficiency–mediated apoptosis should be involved in age-dependent kidney dysfunction through loss of PTCs, and Sirt1-mediated cell adaptation to hypoxia is essential for the CR-mediated kidney protection.

A recent study reported that Sirt1 regulates autophagy through deacetylation of certain molecules associated with autophagy under starvation, but not hypoxia (48). However, how the autophagic machinery selectively destroys damaged mitochondria remains elusive. A study showed that Bnip3 selectively and positively regulates hypoxia-induced mitochondrial autophagy through the disruption of bcl2-beclin1 interaction (15), suggesting that Sirt1-Foxo3 pathway–mediated Bnip3 overexpression may be the regulatory mechanism through which the autophagic machinery selectively destroys damaged mitochondria under hypoxia.

Nuclear translocation of Foxo3 is negatively regulated by PI3K-Akt–mediated phosphorylation (40) and positively by oxidative stress (37, 49). Under AL serum, phosphorylated Foxo3 showed cytoplasmic distribution at the early phase of hypoxia, which suppressed hypoxia-induced autophagy and increased oxidative stress. In contrast, during the late phase of hypoxia under AL serum, Foxo3 translocated into the nucleus in response to oxidative stress, resulting in Foxo3-mediated apoptosis through Bim expression, and this process was enhanced by PI3K inhibition. Thus, under hypoxia in AL serum, the PI3K-Akt pathway plays a biphasic role, increasing mitochondrial oxidative stress through inhibition of autophagy and suppressing Foxo3-mediated apoptosis under oxidative stress. These findings are in agreement with the notion that acceleration of the insulin-PI3K-Akt pathway enhances the aging process (50), but has an antiapoptotic effect against hypoxia (51) and oxidative stress (40). Furthermore, Sirt1 attenuated PI3K inhibition–mediated acceleration of apoptosis under AL serum, which suggests that Sirt1, rather than PI3K, plays a central role for cell survival in the aging process.

Foxo3 promotes resistance to certain stress (37, 52), whereas it promotes apoptosis under other stress (40). However, how Foxo3 selects the exact target gene in response to a specific condition remains obscure. In this study, under CR serum, Foxo3 was deacetylated by Sirt1 and bound to p27Kip1 and Bnip3 promoter, resulting in cell adaptation to hypoxia. In contrast, acetylated Foxo3 enhanced hypoxia-related apoptosis through Bim overexpression under AL serum. A prior report suggested that Sirt1 regulates Foxo3 transcriptional activity under oxidative stress to promote cell survival (37). In addition to this, our results provide further evidence that Sirt1-mediated deacetylation of Foxo3 is essential for cell survival and the mechanism by which Foxo3 selects a specific gene promoter.

The present study demonstrated that mitochondrial damage in aged kidney is associated with Sirt1 deficiency and that Sirt1 promotes cell adaptation to hypoxia through autophagy in aged kidney. Our results provide what we believe to be the first evidence that Sirt1, the PI3K-Akt pathway, and Foxo3 coordinately regulate age-dependent tissue dysfunction and autophagy in mammals, as previously reported in lower organisms (23, 24, 53, 54). The reduced autophagy in the kidney may be involved in the age-associated weakness of PTCs against various renal toxicities, such as drug toxicity and proteinuria in glomerular diseases. Autophagy is currently the focus of research in various fields, such as aging (55), metabolic diseases (56, 57), and immune diseases (58). Our concept should be helpful in the design of studies aiming to further explore autophagy-related diseases and lead to the establishment of new therapies that can delay the progression of hypoxia- and age-related tissue dysfunction, including CKD in elderly patients.

## Methods

*Study approval.* The Research Center for Animal Life Science of Shiga University of Medical Science approved all animal experiments.

*Reagents and materials.* Anti-LC3 and anti-Hif1a were purchased from NOVUS Biologicals. Anti-Sqstm1/p62 was from Progen. Anti–nucleoporine p62 was from BD Biosciences. Anti-beclin1, anti-p27Kip1, and anti-Bcl2 was from Santa Cruz Biotechnology Inc. Anti-Sirt1 was from Upstate Cell Signaling. Anti-GAPDH was from Chemicon. Anti-Bnip3, anti-pFoxo3 (Ser253), anti-Foxo3, anti–cleaved caspase 3, anti-PARP, and anti-acetyllysine were from Cell Signaling Technology. Anti-8OHdG was from Japan

Institute for the Control of Aging. Hypoxyprobe-1 kit was obtained from Natural Pharmacia International Inc. Anti-β-actin, E64d, pepstatin A, LY294002, and NAC were from Sigma-Aldrich.

*CR in aged mice.* Experiments were performed essentially as described previously (59). Male C57BL/6 mice were obtained from CLEA Japan. Six-week-old mice were maintained on a 12-hour light/12-hour dark cycle and provided food and water AL for 12 months. At 12 months of age, they were divided into 2 groups: AL and CR ($n$ = 10 per group). During the following 12 months, mice of the CR group were fed an amount of food corresponding to 60% of the amount of food consumed by the AL group. Food consumption was measured every 2 weeks, and the results were used to calculate the daily food intake. Finally, the 24-month-old (aged) AL and CR mice and the 3-month-old (young) mice were sacrificed (60).

*CR in Sirt1$^{+/-}$ mice.* The *Sirt1* mouse strain on SV129 background were provided by F.W. Alt (Harvard University, Boston, Massachusetts; ref. 61). Male *Sirt1*$^{+/-}$ mice and their WT littermates were provided food and water AL for 6 months. At 6 months of age, they were divided into 3 groups — WT mice with AL ($n$ = 6), *Sirt1*$^{+/-}$ mice with AL ($n$ = 10), and *Sirt1*$^{+/-}$ mice with CR ($n$ = 10) — and followed for the next 6 months. During the 6-month observation period, 1 WT mouse, 3 *Sirt1*$^{+/-}$ mice with AL, and 3 *Sirt1*$^{+/-}$ mice with CR died from neoplasia. Finally, at 12 months of age, we sacrificed 5 WT control mice, 7 *Sirt1*$^{+/-}$ AL mice, and 7 *Sirt1*$^{+/-}$ CR mice.

*Serum cystatin C and urinary albumin level.* Serum cystatin C was determined using Cystatin C (mouse) ELISA Kit (ALEXIS Biochemicals). Urinary albumin excretion was measured with a mouse-specific sandwich ELISA system (Albuwell; Exocell) and was expressed as the total amount excreted in 24 hours (60).

*Histopathological examination.* For semiquantitative evaluation of the fibrotic and 8-OHdG scores, 20 randomly selected glomerulus or tubulointerstitial areas per mouse were graded in a double-blind manner, as reported previously (60), with minor modifications.

*Quantitative RT-PCR.* Isolation of total RNA from kidney, and determination of cDNA synthesis by reverse transcription and quantitative real-time PCR were performed as described previously (60). The sequences of the primers are provided in Supplemental Table 3.

*EM.* Parts of the removed kidneys were cut into small tissue blocks (1 $mm^3$), and fixed in 2.0% glutaraldehyde and 2.0% paraformaldehyde with 0.1 mol/l phosphate buffer at 4°C. After fixation with 2% osmium tetroxide, tissues were dehydrated in a series of graded ethanol solutions, ethanol was substituted with propylene oxide, and then embedded in epoxy resin. Ultrathin sections were double-stained with uranyl acetate and lead. Sections were examined under a JEM1200EX EM (JOEL) at 80 kV.

*Cells.* Mouse renal PTCs were cultured as described previously (62). Sera from aged AL and CR rats (60% of AL for 12 months) were obtained and used as described previously (20, 38, 39). After 24 hours of starvation with serum-free DMEM, the cultured PTCs grown in the presence of serum from CR or AL animals for 6 hours were exposed to hypoxia (1% $O_2$) under the indicated conditions.

*Transient transfection of siRNA.* siRNA for control and siRNA for Foxo3 were purchased from Ambion. Transient transfection of siRNA was performed using Lipofectamine 2000 (Invitrogen) (63). Hypoxic studies were performed after 24 hours of siRNA transfection.

*Plasmids and viral infection.* For the production of retrovirus, full-length cDNA of mouse *Bnip3* was amplified by PCR, subcloned into pCR-TOPO II vectors (Invitrogen), and inserted into pBABE vectors. pBABE-Sirt1, pSUPER-siSirt1, and pSUPER-siBnip3 were provided by L. Guarente (Massachusetts Institute of Technology, Cambridge; ref. 64) and by K. Inoki (University of Michigan, Ann Arbor). The indicated retrovirus vectors were generated and infected into cells as reported previously (63). Adenovirus for Sirt1 was provided by T. Kitamura and T. Sasaki (Gunma University, Maebashi, Japan).

*IP and IB.* Homogenates of whole kidney and PTCs in lysis buffer containing nicotinamide were mixed with Foxo3 antibody and followed by the addition of protein A/G–Sepharose. IP and IB were performed as described previously (63).

*In vitro autophagy assays.* Autophagy was visualized in cultured PTCs by transfection of GFP-LC3 (cDNA of LC3 was provided by T. Yoshimori, Osaka University, Japan, and N. Mizushima, Tokyo Medical and Dental University, Japan; refs. 32, 33). To detect autophagy by Western blot analysis, the indicated cells were treated with E64d and pepstatin A to inhibit lysosomal enzyme activity (33).

*ChIP assay.* The ChIP experiments on kidney samples or PTCs were performed using the ChIP-IT kit from Active Motif according to the instructions provided by the manufacturer. Primer sequences are listed in Supplemental Table 3.

*Immunofluorescent study.* To detect hypoxic conditions in each group of mice, a chemical probe for hypoxia, pimonidazole (Belmont), was injected intraperitoneally 1 hour before sacrifice. For immunofluorescence staining, we incubated frozen kidney sections with antibodies against pimonidazole and Bnip3 or LC3. The cultured PTCs were fixed with acetone for 10 minutes and incubated with antibodies against Sirt1 and Foxo3 after blocking with 2% BSA in PBS, using the protocols described previously (63).

*8-OHdG levels, point mutation, and deletion mutation in mtDNA.* The mtDNA was extracted from the kidney using the mtDNA Extractor CT kit (Wako). The 8-OHdG levels in DNase I–digested mtDNA were determined by ELISA (Japan Institute for the Control of Aging; ref. 65). To determine the sequence of cytochrome *b* gene in mtDNA, we amplified its coding region with Pfu-ultra polymerase (Invitrogen) using the primers listed in Supplemental Table 3. The PCR-amplified fragments were subcloned into TOPO TA cloning kit (Invitrogen) and sequenced with the M13 primer (65). We assayed a common deletion mutation, D-17 (28), in mtDNA using quantitative PCR with primers flanking the D-17 deletion and with template mtDNAs cut at an *Mlu*I site present in the region deleted in D-17 (65). The sequences of primers for the normal and D-17–deleted cytochrome *b* gene are provided in Supplemental Table 3.

*NAD content.* NAD content was determined using the NAD/NADH Quantitation Kit (BioVision) and the protocol supplied by the manufacturer.

*Statistics.* All values are expressed as mean ± SEM. Differences among multiple data sets were analyzed by 1- or 2-way ANOVA, followed by Scheffé's test. Statistical analyses of correlations were performed with the JMP program (version 5.0; SAS Institute Japan). The distribution of variables was analyzed by checking the data histograms, and normal distribution was tested by the Kolmogorov-Smirnov and Shapiro-Wilk tests. Pearson correlation coefficients were calculated to investigate the association among the indicated parameters. In all analyses, a $P$ value less than 0.05 denoted the presence of a statistically significant difference.

## Acknowledgments

We thank L. Guarente (Massachusetts Institute of Technology, Cambridge) and K. Inoki (University of Michigan, Ann Arbor) for helpful discussions and providing materials and H. Inoue, T. Yoshizaki, and M. Sera (Shiga University of Medical Science) and the Central Research Laboratory of Shiga University of Medical Science for valuable technical assistance. We also thank T. Kitamura and T. Sasaki (Gunma University, Japan), T. Yoshimori (Osaka University, Japan), and N. Mizushima (Tokyo Medical and Dental University, Japan) for providing materials and Frederick W. Alt (Harvard University, Cambridge) and S. Ezoe (Osaka University) for the *Sirt1*$^{+/-}$ mouse strain. S. Kume is a Research Fellow of the Japan Society for the Promotion of Science (JSPS). This study was supported by a Grant-in-Aid for JSPS Fellows to S. Kume, Grants-

in-Aid for Scientific Research to D. Koya, and a grant from the Uehara Memorial Foundation to D. Koya.
Received for publication October 8, 2009, and accepted in revised form January 20, 2010.

Address correspondence to: Daisuke Koya, Division of Endocrinology and Metabolism, Kanazawa Medical University, Uchinada-Cho, Kahoku-Gun, Ishikawa 920-0293, Japan. Phone: 81.76.286.2211; Fax: 81.76.286.6927; E-mail: koya0516@kanazawa-med.ac.jp.

1. Baylis C, Corman B. The aging kidney: insights from experimental studies. *J Am Soc Nephrol.* 1998; 9(4):699–709.
2. Coresh J, Astor BC, Greene T, Eknoyan G, Levey AS. Prevalence of chronic kidney disease and decreased kidney function in the adult US population: Third National Health and Nutrition Examination Survey. *Am J Kidney Dis.* 2003;41(1):1–12.
3. Epstein M. Aging and the kidney. *J Am Soc Nephrol.* 1996;7(8):1106–1122.
4. Cutler RG. Human longevity and aging: possible role of reactive oxygen species. *Ann N Y Acad Sci.* 1991; 621:1–28.
5. Droge W. Free radicals in the physiological control of cell function. *Physiol Rev.* 2002;82(1):47–95.
6. Hutter E, Unterluggauer H, Garedew A, Jansen-Durr P, Gnaiger E. High-resolution respirometry--a modern tool in aging research. *Exp Gerontol.* 2006; 41(1):103–109.
7. Yowe DL, Ames BN. Quantitation of age-related mitochondrial DNA deletions in rat tissues shows that their pattern of accumulation differs from that of humans. *Gene.* 1998;209(1–2):23–30.
8. Inoue S, Ishikawa K, Nakada K, Sato A, Miyoshi H, Hayashi J. Suppression of disease phenotypes of adult mito-mice carrying pathogenic mtDNA by bone marrow transplantation. *Hum Mol Genet.* 2006;15(11):1801–1807.
9. Rotig A. Renal disease and mitochondrial genetics. *J Nephrol.* 2003;16(2):286–292.
10. Nohl H, Staniek K, Gille L. Imbalance of oxygen activation and energy metabolism as a consequence or mediator of aging. *Exp Gerontol.* 1997; 32(4–5):485–500.
11. Roberts EL Jr, Chih CP, Rosenthal M. Age-related changes in brain metabolism and vulnerability to anoxia. *Adv Exp Med Biol.* 1997;411:83–89.
12. Pepe S. Mitochondrial function in ischaemia and reperfusion of the ageing heart. *Clin Exp Pharmacol Physiol.* 2000;27(9):745–750.
13. Nangaku M, Inagi R, Miyata T, Fujita T. Hypoxia and hypoxia-inducible factor in renal disease. *Nephron Exp Nephrol.* 2008;110(1):e1–e7.
14. Chandel NS, Budinger GR. The cellular basis for diverse responses to oxygen. *Free Radic Biol Med.* 2007;42(2):165–174.
15. Zhang H, et al. Mitochondrial autophagy is an HIF-1-dependent adaptive metabolic response to hypoxia. *J Biol Chem.* 2008;283(16):10892–10903.
16. Kim H, Lee DK, Choi JW, Kim JS, Park SC, Youn HD. Analysis of the effect of aging on the response to hypoxia by cDNA microarray. *Mech Ageing Dev.* 2003;124(8–9):941–949.
17. Serebrovskaya TV, et al. Geriatric men at altitude: hypoxic ventilatory sensitivity and blood dopamine changes. *Respiration.* 2000;67(3):253–260.
18. Masoro EJ. Caloric restriction and aging: an update. *Exp Gerontol.* 2000;35(3):299–305.
19. Weindruch R, Sohal RS. Seminars in medicine of the Beth Israel Deaconess Medical Center. Caloric intake and aging. *N Engl J Med.* 1997;337(14):986–994.
20. Lopez-Lluch G, et al. Calorie restriction induces mitochondrial biogenesis and bioenergetic efficiency. *Proc Natl Acad Sci U S A.* 2006;103(6):1768–1773.
21. McKiernan SH, et al. Adult-onset calorie restriction delays the accumulation of mitochondrial enzyme abnormalities in aging rat kidney tubular epithelial cells. *Am J Physiol Renal Physiol.* 2007; 292(6):F1751–F1760.
22. Kim HJ, Jung KJ, Yu BP, Cho CG, Choi JS, Chung HY. Modulation of redox-sensitive transcription factors by calorie restriction during aging. *Mech Ageing Dev.* 2002;123(12):1589–1595.
23. Kaeberlein M, Andalis AA, Fink GR, Guarente L. High osmolarity extends life span in Saccharomyces cerevisiae by a mechanism related to calorie restriction. *Mol Cell Biol.* 2002;22(22):8056–8066.
24. Lin SJ, Defossez PA, Guarente L. Requirement of NAD and SIR2 for life-span extension by calorie restriction in Saccharomyces cerevisiae. *Science.* 2000; 289(5487):2126–2128.
25. Guarente L, Picard F. Calorie restriction--the SIR2 connection. *Cell.* 2005;120(4):473–482.
26. Michan S, Sinclair D. Sirtuins in mammals: insights into their biological function. *Biochem J.* 2007; 404(1):1–13.
27. Michikawa Y, Mazzucchelli F, Bresolin N, Scarlato G, Attardi G. Aging-dependent large accumulation of point mutations in the human mtDNA control region for replication. *Science.* 1999; 286(5440):774–779.
28. Tanhauser SM, Laipis PJ. Multiple deletions are detectable in mitochondrial DNA of aging mice. *J Biol Chem.* 1995;270(42):24769–24775.
29. Mizushima N. Autophagy: process and function. *Genes Dev.* 2007;21(22):2861–2873.
30. Bjorkoy G, et al. p62/SQSTM1 forms protein aggregates degraded by autophagy and has a protective effect on huntingtin-induced cell death. *J Cell Biol.* 2005;171(4):603–614.
31. Nakai A, et al. The role of autophagy in cardiomyocytes in the basal state and in response to hemodynamic stress. *Nat Med.* 2007;13(5):619–624.
32. Kabeya Y, et al. LC3, a mammalian homologue of yeast Apg8p, is localized in autophagosome membranes after processing. *EMBO J.* 2000;19(21):5720–5728.
33. Klionsky DJ, et al. Guidelines for the use and interpretation of assays for monitoring autophagy in higher eukaryotes. *Autophagy.* 2008;4(2):151–175.
34. Hamacher-Brady A, et al. Response to myocardial ischemia/reperfusion injury involves Bnip3 and autophagy. *Cell Death Differ.* 2007;14(1):146–157.
35. Tracy K, et al. BNIP3 is an RB/E2F target gene required for hypoxia-induced autophagy. *Mol Cell Biol.* 2007;27(17):6229–6242.
36. Mammucari C, et al. FoxO3 controls autophagy in skeletal muscle in vivo. *Cell Metab.* 2007; 6(6):458–471.
37. Brunet A, et al. Stress-dependent regulation of FOXO transcription factors by the SIRT1 deacetylase. *Science.* 2004;303(5666):2011–2015.
38. Cohen HY, et al. Calorie restriction promotes mammalian cell survival by inducing the SIRT1 deacetylase. *Science.* 2004;305(5682):390–392.
39. de Cabo R, Furer-Galban S, Anson RM, Gilman C, Gorospe M, Lane MA. An in vitro model of caloric restriction. *Exp Gerontol.* 2003;38(6):631–639.
40. Brunet A, et al. Akt promotes cell survival by phosphorylating and inhibiting a Forkhead transcription factor. *Cell.* 1999;96(6):857–868.
41. Medema RH, Kops GJ, Bos JL, Burgering BM. AFX-like Forkhead transcription factors mediate cell-cycle regulation by Ras and PKB through p27kip1. *Nature.* 2000;404(6779):782–787.
42. Essafi A, et al. Direct transcriptional regulation of Bim by FoxO3a mediates STI571-induced apoptosis in Bcr-Abl-expressing cells. *Oncogene.* 2005; 24(14):2317–2329.
43. Anderson RM, Bitterman KJ, Wood JG, Medvedik O, Sinclair DA. Nicotinamide and PNC1 govern lifespan extension by calorie restriction in Saccharomyces cerevisiae. *Nature.* 2003;423(6936):181–185.
44. Lin SJ, Ford E, Haigis M, Liszt G, Guarente L. Calorie restriction extends yeast life span by lowering the level of NADH. *Genes Dev.* 2004;18(1):12–16.
45. Bordone L, et al. SIRT1 transgenic mice show phenotypes resembling calorie restriction. *Aging Cell.* 2007;6(6):759–767.
46. Boily G, et al. SirT1 regulates energy metabolism and response to caloric restriction in mice. *PLoS One.* 2008;3(3):e1759.
47. Higami Y, Shimokawa I. Apoptosis in the aging process. *Cell Tissue Res.* 2000;301(1):125–132.
48. Lee IH, et al. A role for the NAD-dependent deacetylase Sirt1 in the regulation of autophagy. *Proc Natl Acad Sci U S A.* 2008;105(9):3374–3379.
49. Marinkovic D, et al. Foxo3 is required for the regulation of oxidative stress in erythropoiesis. *J Clin Invest.* 2007;117(8):2133–2144.
50. Bartke A. Insulin and aging. *Cell Cycle.* 2008; 7(21):3338–3343.
51. Brunelle JK, Chandel NS. Oxygen deprivation induced cell death: an update. *Apoptosis.* 2002;7(6):475–482.
52. Mei Y, Zhang Y, Yamamoto K, Xie W, Mak TW, You H. FOXO3a-dependent regulation of Pink1 (Park6) mediates survival signaling in response to cytokine deprivation. *Proc Natl Acad Sci U S A.* 2009; 106(13):5153–5158.
53. Ogg S, et al. The Fork head transcription factor DAF-16 transduces insulin-like metabolic and longevity signals in *C. elegans*. *Nature.* 1997;389(6654):994–999.
54. Sigmond T, et al. Autophagy in *Caenorhabditis elegans*. *Methods Enzymol.* 2008;451:521–540.
55. Zhang C, Cuervo AM. Restoration of chaperone-mediated autophagy in aging liver improves cellular maintenance and hepatic function. *Nat Med.* 2008;14(9):959–965.
56. Ebato C, et al. Autophagy is important in islet homeostasis and compensatory increase of beta cell mass in response to high-fat diet. *Cell Metab.* 2008;8(4):325–332.
57. Singh R, et al. Autophagy regulates lipid metabolism. *Nature.* 2009;458(7242):1131–1135.
58. Sanjuan MA, et al. Toll-like receptor signalling in macrophages links the autophagy pathway to phagocytosis. *Nature.* 2007;450(7173):1253–1257.
59. Piper MD, Bartke A. Diet and aging. *Cell Metab.* 2008;8(2):99–104.
60. Kume S, et al. Role of altered renal lipid metabolism in the development of renal injury induced by a high-fat diet. *J Am Soc Nephrol.* 2007;18(10):2715–2723.
61. Cheng HL, et al. Developmental defects and p53 hyperacetylation in Sir2 homolog (SIRT1)-deficient mice. *Proc Natl Acad Sci U S A.* 2003; 100(19):10794–10799.
62. Takaya K, et al. Involvement of ERK pathway in albumin-induced MCP-1 expression in mouse proximal tubular cells. *Am J Physiol Renal Physiol.* 2003; 284(5):F1037–F1045.
63. Kume S, et al. SIRT1 inhibits transforming growth factor beta-induced apoptosis in glomerular mesangial cells via Smad7 deacetylation. *J Biol Chem.* 2007;282(1):151–158.
64. Picard F, et al. Sirt1 promotes fat mobilization in white adipocytes by repressing PPAR-gamma. *Nature.* 2004;429(6993):771–776.
65. Kakoki M, et al. Senescence-associated phenotypes in Akita diabetic mice are enhanced by absence of bradykinin B2 receptors. *J Clin Invest.* 2006; 116(5):1302–1309.

Biochemical and Biophysical Research Communications 402 (2010) 265–271

Contents lists available at ScienceDirect

Biochemical and Biophysical Research Communications

journal homepage: www.elsevier.com/locate/ybbrc

# Oleate and eicosapentaenoic acid attenuate palmitate-induced inflammation and apoptosis in renal proximal tubular cell

Mariko Soumura [a], Shinji Kume [a], Keiji Isshiki [a], Naoko Takeda [a], Shin-ichi Araki [a], Yuki Tanaka [a], Toshiro Sugimoto [a], Masami Chin-Kanasaki [a], Yoshihiko Nishio [a], Masakazu Haneda [b], Daisuke Koya [c], Atsunori Kashiwagi [a], Hiroshi Maegawa [a], Takashi Uzu [a,*]

[a] Department of Medicine, Shiga University of Medical Science, Seta, Otsu, Shiga 520-2192, Japan
[b] Department of Medicine, Asahikawa Medical College, Asahikawa, Hokkaido, Japan
[c] Department of Medicine, Kanazawa Medical University, Kahoku-Gun, Ishikawa, Japan

ARTICLE INFO

*Article history:*
Received 29 September 2010
Available online 16 October 2010

*Keywords:*
Renal lipotoxicity
PKCθ
Inflammation
Apoptosis
Free fatty acid
Dgat2

ABSTRACT

Free fatty acid (FFA)-bound albumin, which is filtrated through the glomeruli and reabsorbed into proximal tubular cells, is one of the crucial mediators of tubular damage in proteinuric kidney disease. In this study, we examined the role of each kind of FFA on renal tubular damage *in vitro* and tried to identify its molecular mechanism. In cultured proximal tubular cells, a saturated fatty acid, palmiate, increased the expression of monocyte chemoattractant protein-1 (MCP-1), but this effect was abrogated by co-incubation of monounsaturated fatty acid, oleate, or ω-3 polyunsaturated fatty acid, eicosapentaenoic acid (EPA). Palmitate led to intracellular accumulation of diacylglycerol (DAG) and subsequent activation of protein kinase C protein family. Among the several PKC inhibitors, rottlerin, a PKCθ inhibitor, prevented palmitate-induced MCP-1 expression via inactivation of NFB pathway. Overexpression of dominant-negative PKCθ also inhibited palmitate-induced activation of MCP-1 promoter. Furthermore, palmitate enhanced PKCθ-dependent mitochondrial apoptosis, which was also prevented by co-incubation with oleate or EPA through restoration of pro-survival Akt pathway. Moreover, oleate and EPA inhibited palmitate-induced PKCθ activation through the conversion of intracellular DAG to triglyceride with the restoration of diacylglycerol acyltransferase 2 expression. These results suggest that oleate and EPA have protective effects against the palmitate-induced renal tubular cell damage by inhibiting PKCθ activation.


## 1. Introduction

In proteinuric kidney disease, lipotoxicity has been proposed as a pathogenic mechanism of progressive renal tubulointerstitial damage [1–3], which correlates with renal prognosis [4]. Serum free fatty acids (FFAs) bound to albumin are filtered through the glomeruli, reabsorbed by the proximal tubular cells and followed by their metabolism. Several experimental studies using FFA-bound albumin-overload animal models have shown that excess FFA-load in proteinuria induces severe tubulointerstitial injury consisting of inflammatory cell infiltration and renal tubular cell apoptosis [1–3].

Serum FFAs are composed of saturated fatty acids, monounsaturated fatty acids and polyunsaturated fatty acids, and this composition is modified by metabolic state such as metabolic syndrome and obese [5], which may affect renal prognosis. However, at present, the contribution of the composite change in serum FFA to tubulointerstitial damage remains unclear. Therefore, understanding the effect and mechanism of each type of FFA on tubular cell damage should provide a new therapeutic strategy to improve renal prognosis of obese or diabetic patients with overt proteinuria.

Several molecular pathways are involved in FFAs-mediated tissue or cell dysfunction [6–8]. Among these, recent studies have shown that accumulation of FFAs-mediated diacylglycerol (DAG) contributes to the activation of protein kinase C isoforms (PKCs) and subsequent tissue impairments [9,10]. PKCs are divided into classified into conventional, novel, and atypical subfamilies, and several of these have been identified in the kidney. However, until recently, there are no studies on the contribution of each kind of PKC to the FFA-mediated tubular damage.

In the present study, we evaluated the effects and molecular mechanism of saturated FFA (palmitate), monounsaturated FFA (oleate), and ω-3 polyunsaturated FFA (eicosapentaenoic acid;

*Abbreviations:* MCP-1, monocyte chemoattractant protein-1; EPA, eicosapentaenoic acid; DAG, diacylglycerol; FFA, free fatty acid; SFA, saturated fatty acid; MUFA, monounsaturated fatty acid; PUFAs, polyunsaturated fatty acids; TNFα, tumor necrosis factor-α; LPS, lipopolysaccharide; PKC, protein kinase C; mPTEC, mouse proximal tubular epithelial cell; LDs, lipid droplets; Dgat, diacylglycerol acyltransferase; TLRs, Toll-like receptors; hPTEC, human proximal tubular epithelial cell.

* Corresponding author. Fax: +81 775 43 3858.
*E-mail address:* takuzu@belle.shiga-med.ac.jp (T. Uzu).

0006-291X/$ - see front matter © 2010 Elsevier Inc. All rights reserved.
doi:10.1016/j.bbrc.2010.10.012

EPA) on the expression of monocyte chemoattractant protein-1 (MCP-1) and apoptosis in cultured proximal tubular cells, with a special focus on FFA-mediated PKCs activation.

## 2. Materials and methods

### 2.1. Materials

Bovine serum albumin (BSA; fatty acid free, fraction V) was obtained from Nacalai Tesque (Kyoto, Japan). BSA did not contain a high level of endotoxin (<3.0 ng/ml), as confirmed by the Endospacy method (FALCO, Kyoto, Japan). Anti-PARP, anti-cleaved caspase 3, anti-phospho-PKCθ(Thr$^{538}$), anti-PKC, anti-phospho-PKCμ(Ser$^{916}$), anti-phospho-PKCδ(Thr$^{505}$), anti-PKCδ, anti-phospho-PKCβII(Ser$^{660}$), anti-phospho-PKCα/βII(Thr$^{638/641}$), anti-phospho-PKCζ/λ(Thr$^{410/403}$), anti-phospho-p44/p42 MAPK(Thr$^{202}$/Tyr$^{204}$), anti-phospho-p38 MAPK(Thr$^{180}$/Tyr$^{182}$), anti-phospho-IκBα(Ser176/$^{180}$), anti-phospho-JNK(Thr$^{183}$/Tyr$^{185}$), anti-p44/p42 MAPK, anti-p38 MAPK, anti-IκBα, anti-Bad, anti-phospho-Bad(Ser$^{136}$), anti-histone, anti-phospho-Akt(Ser$^{473}$) and anti-JNK antibodies were purchased from Cell Signalling Technology (Beverly, MA). Anti-Akt, anti-PKCα, anti-PKCζ/λ and anti-PKCβII antibodies were from Santa Cruz Biotechnology (Santa Cruz, CA). Rottlerin, GÖ6850, GÖ6976, and GÖ6983 were purchased from Calbiochem (San Diego, CA). Plasmid vectors encoding the mouse PKCβII, PKCμ, PKCδ, and PKCθ were kindly provided by Dr. A. Reifel Miller (Lilly Research Laboratories, Indianapolis, IN) [11]. Wild-type PKCθ and mutated PKCθ(K/R) and (A/E) were kindly provided by Dr. Gottfried Baier (Innsbruck Medical University, Innsbruck, Austria) [12].

### 2.2. Cell culture

Mouse proximal tubular epithelial cells (mPTEC) were cultured as described [13]. Primary human proximal tubular epithelial cells (hPTEC) were purchased from Primary Cell Co., Ltd. (Hokkaido, Japan). Lipid-containing media were prepared by conjugation of FFA with FFA-free bovine serum albumin. Briefly, sodium palmitate (Sigma, St. Louis, MO), oleic acid (Sigma), eicosapentaenoic acid

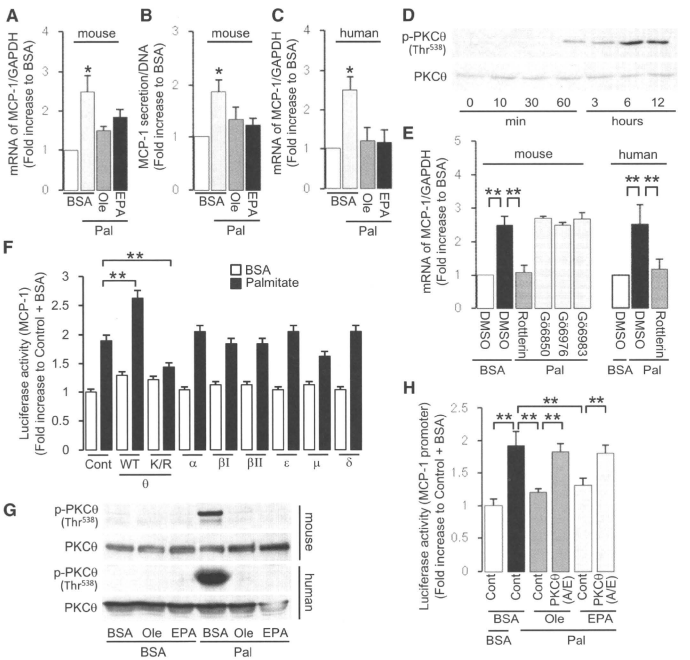


**Fig. 1.** Oleate and EPA abrogate palmitate-induced MCP-1 expression through the inhibition of PKCθ in renal tubular cell. (A) mRNA expression of MCP-1 in mPTEC incubated with 150 μM of palmitate and supplemented with either 150 μM oleate or 50 μM EPA. (B) MCP-1 secretion in the culture medium, determined by ELISA, incubated for 18 h in the presence of different FFAs. (C) mRNA expression in hPTEC incubated with palmitate (150 μM) and supplemented with either 150 μM oleate or 50 μM EPA. (D) Immunoblot showing phosphorylation of PKCθ in mPTEC exposed to palmitate (150 μM). (E) mRNA expression of MCP-1 in mPTEC and hPTEC exposed to palmitate (150 μM) for 12 h in the presence of each PKCs inhibitor. Rottlerin; PKCθ and δ inhibitor, Gö6850; PKCα, βI, βII, γ, δ and ε inhibitor, Gö6976; PKCα, βI and μ inhibitor, Gö6983: PKCα, βI, βII, γ, δ and ζ/λ inhibitor. (F) MCP-1 promoter activity in each PKCs overexpression vector-transfected mPTEC under treatment with palmitate (150 μM) for 12 h. Data were expressed as fold increase to BSA + Control vector. (G) Immunoblot showing phosphorylation of PKCθ in mPTEC and hPTEC exposed to palmitate (150 μM) for 6 h in the presence of either oleate (150 μM) or EPA (50 μM). (H) MCP-1 promoter activity in mutated PKCθ(A/E)-transfected mPTEC under treatment with palmitate (150 μM) for 12 h, supplemented with oleate or EPA. All data are expressed as mean ± SD of three independent experiments. $^{*}P < 0.01$ vs. other groups. $^{**}P < 0.05$ vs. indicated groups. WT; wild type of PKCθ. K/R; dominant-negative mutated PKCθ. A/E; constitutive-active mutated PKCθ.

(Cayman Chemical, Ann Arbor, MI) were dissolved in 50% ethanol, mixed vigorously with FFA-free BSA in phosphate-buffered saline (PBS). BSA was used as control. For experiments using inhibitors, the cells were incubated with the indicated PKC inhibitors for 60 min prior to exposure to palmitate.

### 2.3. Measurements of mRNA levels

The mRNA levels were assessed by real-time PCR [14]. Total RNA was isolated by using the TRIzol protocol and cDNA was synthesized by reverse transcriptional PCR as described [14]. Primer sets were as follows: MCP-1, 5′-GCCCCACTCACCTGCTGCTACT-3′ and 5′-CCTGCTGCTGGTGATCCTCTTGT-3′; Dgat-2, 5′-ATGGGTCCAG AAGAAGTTCCAG-3′ and 5′-GGTGATGGGCTTGGAGTAGG-3′ GAPDH, 5′-ATGGCCTTCCGTGTTCCT-3′ and 5′-GCCTGCTTCACCACCTTCT-3′.

### 2.4. Enzyme-linked immunosorbent assay (ELISA)

Conditioned media were collected and MCP-1 levels were determined using a mouse MCP-1 ELISA kit (Bio-Source, Camarillo, CA) [13].

### 2.5. Isolation of cell fraction and immunoblot analysis

Nuclear and cytosolic proteins were prepared as described previously [13]. Immunoblot analysis was performed as described previously [14].

### 2.6. Transient transfection and luciferase assay

The pGL3-MCP-1 luciferase vector and phRL-null vector were described previously [15]. The mPTEC were transfected with phRL-null and luciferase reporter constructs by LipofectAMINE (Invitrogen, Carlsbad, CA). The cells were incubated with palmitate for 12 h after transfection. Luciferase activity was determined with a luciferase assay kit (Promega, Madison, WI) as described [15]. Small interference RNA against mouse Dgat2 and a control siRNA were utilized (SMARTpool Reagent; Dharmacon, Chicago, IL), and transfected with DharmaFECT 4 Transfection Reagent (Dharmacon).

### 2.7. Mito-PT apoptosis detection kit

Mito-PT apoptosis detection kit (B-Bridge International Inc., San Jose, CA) was used for assessment of apoptosis as the manufacturer's instruction [16]. The fluorescence intensity was measured as described [16].

### 2.8. Determination of total DAG content

Total DAG content in mPTEC cultured in 100-mm dishes was determined by the diacylglycerol kinase method, which quantitatively converts DAG to [$^{32}$P]phosphatidic acid (PA) in the presence of [$\gamma$-$^{32}$P]ATP. Total cellular lipids were extracted according to the methods of Bligh and Dyer [17], and total DAG was measured according to the method using diacylglycerol kinase [18]. The resulting [$^{32}$P]PA was separated and visualized as described [18].

## 3. Results

### 3.1. Oleate and EPA prevent palmitate-induced MCP-1 expression by inhibiting PKCθ activation in proximal tubular cell

We first examined the effects of FFAs on the expression of MCP-1, a pro-inflammatory cytokine, in cultured mPTEC and hPTEC. Treatment with palmitate for 12 h in mPTEC increased MCP-1 mRNA expression in a dose-dependent manner (Supplemental Fig. 1A). Co-incubation with oleate or EPA prevented palmitate-induced mRNA expression and protein secretion of MCP-1in mPTEC (Fig. 1A and B), and this was confirmed in hPTEC (Fig. 1C). Furthermore, EPA, but not oleate, inhibited tumor necrosis factor-α-(TNFα)- and lipopolysaccharide (LPS)-induced MCP-1 expression (Supplemental Fig. 1B and C), suggesting that the anti-inflammatory effect of oleate is specific against palmitate, whereas EPA has global anti-inflammatory effects against various stimuli in proximal tubular cells.

We identified the PKC isoform involved in palmitate-induced MCP-1 expression in renal tubular cells. Palmitate increased phosphorylation of PKCθ(Thr$^{538}$) and PKCμ(Thr$^{401/403}$), but not those of other PKC isoforms (Fig. 1D and Supplemental Fig. 2A). Rottlerin (PKCθ and δ inhibitor), but not the other PKCs inhibitors including PKCμ, significantly suppressed palmitate-induced MCP-1 expression in mPTEC and hPTEC (Fig. 1E). Furthermore, overexpression of wild-type PKCθ, but not the other PKCs, enhanced MCP-1 promoter activity determined by luciferase assay, and overexpression of dominant-negative PKCθ(K/R) inhibited palmitate-induced MCP-1 promoter activation (Fig. 1F).

Co-incubation of oleate or EPA completely prevented phosphorylation of PKCθ(Thr$^{538}$) in palmitate-exposed mPTEC and hPTEC (Fig. 1G). The inhibitory effects of oleate and EPA on palmitate-induced MCP-1 promoter activity were abolished by overexpression of the constitutively active PKCθ(A/E) (Fig. 1H).

### 3.2. Oleate and EPA inhibit palmitate-induced activation of pro-inflammatory PKCθ–NF-κB pathway

PKCs-mediated activation of mitogen-activated protein kinase (MAPKs) or NF-κB pathway has been reported as a critical regulator of PKCs-mediated inflammation [6,7,10]. In fact, we found that palmitate-induced phosphorylation of MAPKs (ERK, p38 and JNK) and IκB, and promoted the nuclear translocation of NF-κB (P65) (Supplemental Fig. 2B). PKCθ inhibitor abolished the palmitate-induced phosphorylation of IκB and nuclear translocation of p65, but

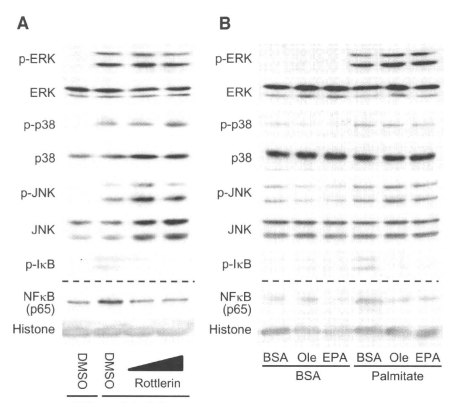


**Fig. 2.** Oleate and EPA inhibit palmitate-induced activation of pro-inflammatory PKCθ–NF-κB pathway. Immunoblot showing phosphorylation of ERK, p38, JNK, IκB, and nuclear p65 in mPTEC exposed to palmitate (150 μM; 10 min for ERK, 6 h for others) co-incubated with (A) rottlerin (PKCθ inhibitor) and (B) oleate (150 μM) or EPA (50 μM).

did not affect palmitate-induced phosphorylations of MAPKs (Fig. 2A). Consistent with this result, both oleate and EPA inhibited palmitate-induced NF-κB activation, but not MAPKs activation (Fig. 2B).

### 3.3. Oleate and EPA prevent palmitate-induced apoptosis by restoring pro-survival effect of Akt in proximal tubular cell

We next examined the effects of FFAs on apoptosis in proximal tubular cells. Incubation with palmitate for 12 h induced cleavages of PARP and caspase 3, indicative of apoptosis (Supplemental Fig. 3A), and co-incubation with oleate or EPA completely prevented this effect in mPTEC and hPTEC (Fig. 3A). These results were confirmed by Mito-PT apoptosis detection kit [16], by which each the living or the dead cells were observed as orange/yellow- or green-colored cells, respectively (Fig. 3B). Both oleate and EPA failed to inhibit TNFα- and LPS-induced apoptosis (Supplemental Fig. 3B and C), suggesting that the anti-apoptotic effects of oleate and EPA are specific against palmitate-induced apoptosis.

We examined the role of PKC isoform in palmitate-induced apoptosis of renal tubular cells. Rottlerin, but not other PKCs inhibitors, inhibited the cleavages of PARP and caspase 3 in palmitate-exposed mPTEC (Fig. 3C). Anti-apoptotic effect of rottlerin was confirmed in hPTEC exposed to palmitate (Fig. 3D). These results were confirmed by Mito-PT apoptosis detection kit (Fig. 3E), suggesting the involvement of PKCθ in palmitate-induced apoptosis.

Furthermore, we examined the downstream pathways of PKCθ to identify further regulatory mechanism(s) of palmitate-induced apoptosis in proximal tubular cells. PKCθ inhibits Akt activation, which causes insulin resistance [19], and Akt has an anti-apoptotic effect against oxidative stress in several types of cells by phosphorylating Bad protein, leading to suppress mitochondrial apoptosis [20]. As expected, we found a significant decrease in Akt phosphorylation at $Ser^{473}$ and Bad phosphorylation at $Ser^{136}$, a phosphorylated site known as a target of Akt, and subsequently an increase in cytosolic cytochrome C after 6 h of palmitate treatment (Supplemental Fig. 3A). These effects were attenuated by pretreatment with rottlerin (Fig. 3F) and co-incubation with oleate or EPA (Fig. 3G).

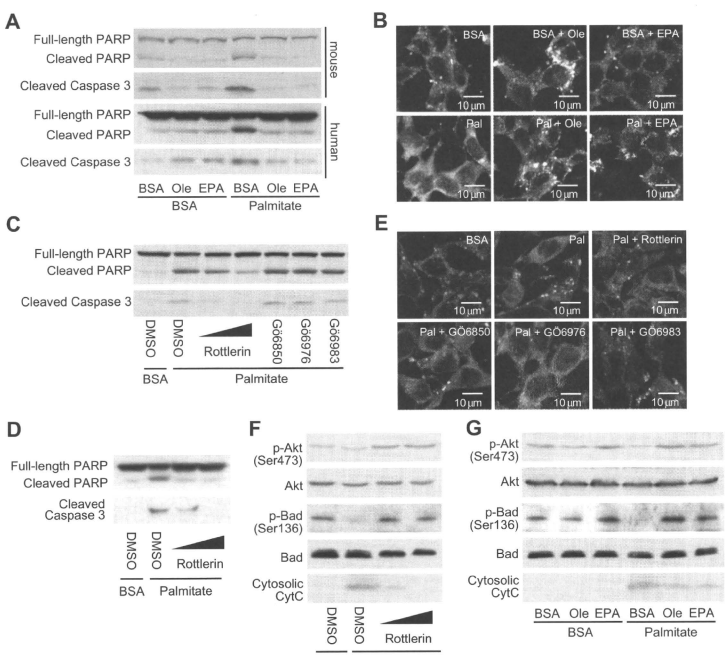


**Fig. 3.** Oleate and EPA prevent palmitate-induced apoptosis through the restoration of Akt activity in renal tubular cell. (A) Immunoblot showing the cleavage of PARP and caspase 3 in mPTEC and hPTEC exposed to palmitate (150 μM) and co-incubated with oleate (150 μM) or EPA (50 μM). (B) Representative photomicrographs showing apoptotic cells incubated with different FFAs for 12 h, determined by Mito-PT apoptosis detection kit. Yellow/orange and green cells indicate living and dead cells, respectively. (C, D) Representative immunoblots showing the cleavage of PARP and caspase 3 in mPTEC (C) and hPTEC (D) exposed to palmitate (150 μM) in the presence of each PKCs inhibitor. Rottlerin; PKCθ and δ inhibitor, Gö6850; PKCα, βI, βII, γ, δ and ε inhibitor, Gö6976; PKCα, βI and μ inhibitor, Gö6983: PKCα, βI, βII, γ, δ and ζ/λ inhibitor. (E) Representative photomicrographs showing apoptotic cells incubated with palmitate (150 μM) in the presence of each PKCs inhibitor, which were determined by Mito-PT apoptosis detection kit. (F, G) Immunoblot showing the phosphorylation of Akt and Bad proteins, and CytC release in mPTEC exposed to palmitate (150 μM; 12 h) co-incubated with (F) rottlerin (PKCθ inhibitor) and (G) oleate (150 μM) or EPA (50 μM). The results were obtained from three independent experiments.

### 3.4. Oleate and EPA reduce palmitate-induced DAG accumulation by promoting TG synthesis through restoration of Dgat2

Because DAG is an allosteric activator of PKCs, we evaluated DAG accumulation in mPTEC incubated with each FFA. Palmitate increased intracellular DAG levels, and co-incubation with oleate or EPA attenuated palmitate-induced DAG accumulation (Fig. 4A). We also analyzed TG accumulation in mPTEC by BODIPY493/503 staining. Lipid droplets (LDs) were hardly visible in palmitate-exposed cells and co-incubation of palmitate-exposed cells with oleate or EPA resulted in marked increase of LDs (Fig. 4B). These differences in the channeling of fatty acids into TG and DAG may be due to changes in the expression of genes involved in TG synthesis. Given that diacylglycerol acyltransferase (Dgat) is the enzyme that catalyzes the final reaction in the synthesis of TG from DAG [21], we assessed the effects of palmitate, oleate and EPA on the expression of this gene. We found that Dgat2 was abundantly expressed, but not Dgat1, in mPTECs (data not shown). Dgat2 mRNA levels were significantly lower in cells exposed to palmitate, and the supplementation with oleate or EPA restored Dgat2 mRNA expression in palmitate-exposed mPTEC (Fig. 4 C). Thus, we finally examined the effect of knockdown of Dgat2 expression on anti-inflammatory and anti-apoptotic effects of oleate and EPA in mPTEC incubated with palmitate. In mPTEC lacking Dgat2 expression (Fig. 4D), both oleate and EPA failed to inhibit palmitate-induced MCP-1 expression (Fig. 4E) and apoptosis (Fig. 4F).

## 4. Discussion

In the current study, we show for the first time that FFAs-induced cell impairments depend on the type of FFA in both human and mouse proximal tubular cells. Palmitate is a mediator of tubular cell damage including inflammation and apoptosis, both of which were reversed by oleate and EPA, suggesting that the altered serum FFA profile could be one of the main causes of severe tubulointerstitial injury seen in the patients with metabolic syndrome and type 2 diabetes. Our results could show first evidence that altered serum FFA profile contributes to renal tubulointerstitial injury.

To identify the molecular mechanism underlying FFAs-mediated tubular cell damages, we focused on DAG-dependent PKCs, since SFAs, including palmitate, increase intracellular DAG levels [10,22]. In the present study, we showed that PKCθ, a novel PKC, plays an important role in FFAs-mediated tubulointerstitial injury including inflammation and apoptosis, and that the degree of PKCθ activation depends on the isoform of FFA and intracellular DAG level. Until recently, palmitate-induced PKCθ activation has been reported to play a major pathological role in insulin resistance [7,10]. We showed here new pathological roles for palmitate-induced PKCθ activation in inflammation and apoptosis in the kidney. We also identified the mechanisms underlying PKCθ-dependent MCP-1 expression, which involved the DAG–PKCθ–NF-κB pathway, but not PKCθ–MAPKs pathway.

The results also showed that the anti-inflammatory effect of oleate was specific for palmitate-induced inflammation, whereas EPA had anti-inflammatory effect not only against palmitate-induced, but also against TNFα- and LPS-induced inflammation. It has been reported that ω-3 PUFA has anti-inflammatory effects by (i) modulation of nuclear receptor activation, i.e., NF-κB suppression [23,24], (ii) metabolic interconversion into biochemical mediators such as resolvins that can counter-regulate inflammation [25,26], (iii) alteration of plasma membrane microorganiza-

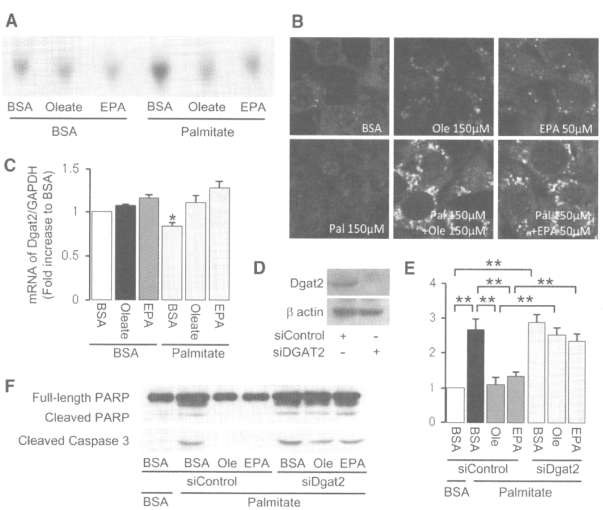


**Fig. 4.** Oleate- and EPA-mediated restoration of Dgat2 expression is required for their renoprotection. (A) DAG accumulation in mPTEC exposed to palmitate (150 μM) for 12 h in the presence with either oleate (150 μM) or EPA (50 μM). (B) Representative photomicrographs of BODIPY493/503 staining to detect intracellular neutral lipid accumulation in mPTEC exposed to palmitate (150 μM) for 12 h in the presence of either oleate (150 μM) or EPA (50 μM). (C) mRNA expression of Dgat2 in mPTEC exposed to palmitate (150 μM) in the presence of either oleate (150 μM) or EPA (50 μM). (D) Immunoblot showing the efficiency of siRNA against Dgat2. (E) Palmitate (150 μM)-induced mRNA expression of MCP-1 in mPTEC transfected with control siRNA or siRNA against Dgat2. (F) Immunoblot showing Palmitate (150 μM)-induced cleavages of PARP and caspase 3 in mPTEC transfected with control siRNA or siRNA against Dgat2. Data are expressed as mean ± SD of three independent experiments. $P < 0.05$ vs. the other groups. * $P < 0.05$ vs. indicated groups.

tion (lipid rafts), particularly as it relates to the function of Toll-like receptors (TLRs), so that ω-3 PUFA acts as a pan-inhibitor of TLRs [27–29]. Our results indicate that oleate does not directly affect NF-κB pathway and the plasma membrane lipid rafts. It can be said that the protective role of oleate against tubulointerstitial injury is limited to lipotoxicity, whereas EPA has a broad protective effect against tubulointerstitial injury.

Our study showed that the anti-apoptotic effects of oleate and EPA were specific against palmitate-induced apoptosis, and that they failed to inhibit TNFα- and LPS-induced apoptosis, suggesting that their anti-apoptotic effects do not depend on inhibition of receptor-mediated cell death pathway, such as FADD-caspase 8 pathway [30,31]. We also found that palmitate-induced PKCθ activation suppressed the pro-survival Akt-pathway, and that oleate and EPA inhibited palmitate-induced apoptosis through the restoration of pro-survival activity of Akt in mPTEC. Thus, our results provided the first evidence for the involvement of PKCθ-mediated Akt inhibition in palmitate-induced mitochondrial apoptosis.

Interestingly, both oleate and EPA attenuated palmitate-induced MCP-1 expression and mitochondrial apoptosis. It is because oleate and EPA counterbalance its toxicity by promoting TG synthesis with restoration of Dgat2 activity, thereby leading to reduced DAG accumulation which is more toxic than TG. Based on these findings, we suggest that channeling FFAs to TG pools through Dgat2 activity in mPTEC can reduce FFA-mediated toxicity, and that this could be employed as a therapeutic target to prevent tubulointerstitial lipotoxicity.

Here, we clearly show the differential role of each kind of FFA in renal injury by using *in vitro* study. In the human study, the concentration of saturated fatty acids in overweight subjects was previously reported to be higher than that in normal-weight subjects (5). Thus, these results suggest that the pharmacological or dietary interventions aiming to correct serum FFA profile may be useful for preventing the progression of renal interstitial injury. However, it is well known that the total concentration of serum unsaturated fatty acids is higher than that of serum saturated fatty acids even in the obese and/or diabetic patients (5). Therefore, further clinical studies are required to clarify whether the relative increase of serum saturated FFA in total FFA actually affects the renal tubulointerstitial injury and the correction of this abnormal FFA profile prevents this injury.

## 5. Conclusion

The present study demonstrated for the first time that oleate and EPA have protective effects against the palmitate-induced renal tubular cell damage by inhibiting PKCθ activation, suggesting that to correct serum FFA profile seems an attractive therapeutic strategy to prevent the progression of tubulointerstitial injury in obese and diabetic patients with chronic kidney diseases.

## Acknowledgments

We thank Dr. A. Reifel Miller (Lilly Research Laboratories, Indianapolis, IN) and Dr. Gottfried Baier (Innsbruck Medical University, Innsbruck, Austria) for the generous gifts of plasmids. We also thank Makiko Sera (Shiga University of Medical Science, Shiga, Japan) for the excellent technical assistance. This work was supported by JSPS KAKENHI to K.I. (21591130).

## Appendix A. Supplementary data

Supplementary data associated with this article can be found, in the online version, at doi:10.1016/j.bbrc.2010.10.012.

## References

[1] M. Arici, R. Chana, A. Lewington, J. Brown, N.J. Brunskill, Stimulation of proximal tubular cell apoptosis by albumin-bound fatty acids mediated by peroxisome proliferator activated receptor-gamma, J. Am. Soc. Nephrol. 14 (2003) 17–27.
[2] A. Kamijo, K. Kimura, T. Sugaya, M. Yamanouchi, H. Hase, T. Kaneko, Y. Hirata, A. Goto, T. Fujita, M. Omata, Urinary free fatty acids bound to albumin aggravate tubulointerstitial damage, Kidney Int. 62 (2002) 1628–1637.
[3] M.E. Thomas, K.P. Harris, J. Walls, P.N. Furness, N.J. Brunskill, Fatty acids exacerbate tubulointerstitial injury in protein-overload proteinuria, Am. J. Physiol. Renal Physiol. 283 (2002) F640–F647.
[4] R.A. Risdon, J.C. Sloper, H.E. De Wardener, Relationship between renal function and histological changes found in renal-biopsy specimens from patients with persistent glomerular nephritis, Lancet 2 (1968) 363–366.
[5] C. Klein-Platat, J. Drai, M. Oujaa, J.L. Schlienger, C. Simon, Plasma fatty acid composition is associated with the metabolic syndrome and low-grade inflammation in overweight adolescents, Am. J. Clin. Nutr. 82 (2005) 1178–1184.
[6] S. Crunkhorn, F. Dearie, C. Mantzoros, H. Gami, W.S. da Silva, D. Espinoza, R. Faucette, K. Barry, A.C. Bianco, M.E. Patti, Peroxisome proliferator activator receptor gamma coactivator-1 expression is reduced in obesity: potential pathogenic role of saturated fatty acids and p38 mitogen-activated protein kinase activation, J. Biol. Chem. 282 (2007) 15439–15450.
[7] M. Jove, A. Planavila, R.M. Sanchez, M. Merlos, J.C. Laguna, M. Vazquez-Carrera, Palmitate induces tumor necrosis factor-alpha expression in C2C12 skeletal muscle cells by a mechanism involving protein kinase C and nuclear factor-kappaB activation, Endocrinology 147 (2006) 552–561.
[8] J.J. Senn, Toll-like receptor-2 is essential for the development of palmitate-induced insulin resistance in myotubes, J. Biol. Chem. 281 (2006) 26865–26875.
[9] S.C. Benoit, C.J. Kemp, C.F. Elias, W. Abplanalp, J.P. Herman, S. Migrenne, A.L. Lefevre, C. Cruciani-Guglielmacci, C. Magnan, F. Yu, K. Niswender, B.G. Irani, W.L. Holland, D.J. Clegg, Palmitic acid mediates hypothalamic insulin resistance by altering PKC-theta subcellular localization in rodents, J. Clin. Invest. 119 (2009) 2577–2589.
[10] T. Coll, E. Eyre, R. Rodriguez-Calvo, X. Palomer, R.M. Sanchez, M. Merlos, J.C. Laguna, M. Vazquez-Carrera, Oleate reverses palmitate-induced insulin resistance and inflammation in skeletal muscle cells, J. Biol. Chem. 283 (2008) 11107–11116.
[11] A.E. Reifel-Miller, D.M. Conarty, K.M. Valasek, P.W. Iversen, D.J. Burns, K.A. Birch, Protein kinase C isozymes differentially regulate promoters containing PEA-3/12-O-tetradecanoylphorbol-13-acetate response element motifs, J. Biol. Chem. 271 (1996) 21666–21671.
[12] B. Bauer, N. Krumbock, F. Fresser, F. Hochholdinger, M. Spitaler, A. Simm, F. Uberall, B. Schraven, G. Baier, Complex formation and cooperation of protein kinase C theta and Akt1/protein kinase B alpha in the NF-kappa B transactivation cascade in Jurkat T cells, J. Biol. Chem. 276 (2001) 31627–31634.
[13] K. Takaya, D. Koya, M. Isono, T. Sugimoto, T. Sugaya, A. Kashiwagi, M. Haneda, Involvement of ERK pathway in albumin-induced MCP-1 expression in mouse proximal tubular cells, Am. J. Physiol. Renal Physiol. 284 (2003) F1037–F1045.
[14] S. Kume, T. Uzu, K. Horiike, M. Chin-Kanasaki, K. Isshiki, S. Araki, T. Sugimoto, M. Haneda, A. Kashiwagi, D. Koya, Calorie restriction enhances cell adaptation to hypoxia through Sirt1-dependent mitochondrial autophagy in mouse aged kidney, J. Clin. Invest. 120 (2010) 1043–1055.
[15] M. Kondo, H. Maegawa, T. Obata, S. Ugi, K. Ikeda, K. Morino, Y. Nakai, Y. Nishio, S. Maeda, A. Kashiwagi, Transcription factor activating protein-2beta: a positive regulator of monocyte chemoattractant protein-1 gene expression, Endocrinology 150 (2009) 1654–1661.
[16] W. Liu, R. Mu, F.F. Nie, Y. Yang, J. Wang, Q.S. Dai, N. Lu, Q. Qi, J.J. Rong, R. Hu, X.T. Wang, Q.D. You, Q.L. Guo, MAC-related mitochondrial pathway in oroxylin-A-induced apoptosis in human hepatocellular carcinoma HepG2 cells, Cancer Lett. 284 (2009) 198–207.
[17] S. Kume, T. Uzu, S. Araki, T. Sugimoto, K. Isshiki, M. Chin-Kanasaki, M. Sakaguchi, N. Kubota, Y. Terauchi, T. Kadowaki, M. Haneda, A. Kashiwagi, D. Koya, Role of altered renal lipid metabolism in the development of renal injury induced by a high-fat diet, J. Am. Soc. Nephrol. 18 (2007) 2715–2723.
[18] K. Isshiki, M. Haneda, D. Koya, S. Maeda, T. Sugimoto, R. Kikkawa, Thiazolidinedione compounds ameliorate glomerular dysfunction independent of their insulin-sensitizing action in diabetic rats, Diabetes 49 (2000) 1022–1032.
[19] Y. Li, T.J. Soos, X. Li, J. Wu, M. Degennaro, X. Sun, D.R. Littman, M.J. Birnbaum, R.D. Polakiewicz, Protein kinase C Theta inhibits insulin signaling by phosphorylating IRS1 at Ser(1 1 0 1), J. Biol. Chem. 279 (2004) 45304–45307.
[20] N.N. Danial, BAD: undertaker by night, candyman by day, Oncogene 27 (Suppl. 1) (2008) S53–S70.
[21] Y. Shi, D. Cheng, Beyond triglyceride synthesis: the dynamic functional roles of MGAT and DGAT enzymes in energy metabolism, Am. J. Physiol. Endocrinol. Metab. 297 (2009) E10–E18.
[22] E. Montell, M. Turini, M. Marotta, M. Roberts, V. Noe, C.J. Ciudad, K. Mace, A.M. Gomez-Foix, DAG accumulation from saturated fatty acids desensitizes insulin

stimulation of glucose uptake in muscle cells, Am. J. Physiol. Endocrinol. Metab. 280 (2001) E229–E237.
[23] H. Li, X.Z. Ruan, S.H. Powis, R. Fernando, W.Y. Mon, D.C. Wheeler, J.F. Moorhead, Z. Varghese, EPA and DHA reduce LPS-induced inflammation responses in HK-2 cells: evidence for a PPAR-gamma-dependent mechanism, Kidney Int. 67 (2005) 867–874.
[24] A. Mishra, A. Chaudhary, S. Sethi, Oxidized omega-3 fatty acids inhibit NF-kappaB activation via a PPARalpha-dependent pathway, Arterioscler. Thromb. Vasc. Biol. 24 (2004) 1621–1627.
[25] C.N. Serhan, N. Chiang, T.E. Van Dyke, Resolving inflammation: dual anti-inflammatory and pro-resolution lipid mediators, Nat. Rev. Immunol. 8 (2008) 349–361.
[26] C.N. Serhan, S. Yacoubian, R. Yang, Anti-inflammatory and proresolving lipid mediators, Annu. Rev. Pathol. 3 (2008) 279–312.
[27] zA. Ishikado, Y. Nishio, K. Yamane, A. Mukose, K. Morino, Y. Murakami, O. Sekine, T. Makino, H. Maegawa, A. Kashiwagi, Soy phosphatidylcholine inhibited TLR4-mediated MCP-1 expression in vascular cells, Atherosclerosis 205 (2009) 404–412.
[28] J.Y. Lee, D.H. Hwang, The modulation of inflammatory gene expression by lipids: mediation through Toll-like receptors, Mol. Cell 21 (2006) 174–185.
[29] J.Y. Lee, K.H. Sohn, S.H. Rhee, D. Hwang, Saturated fatty acids, but not unsaturated fatty acids, induce the expression of cyclooxygenase-2 mediated through Toll-like receptor 4, J. Biol. Chem. 276 (2001) 16683–16689.
[30] S.G. Cho, E.J. Choi, Apoptotic signaling pathways: caspases and stress-activated protein kinases, J. Biochem. Mol. Biol. 35 (2002) 24–27.
[31] A. Strasser, P.J. Jost, S. Nagata, The many roles of FAS receptor signaling in the immune system, Immunity 30 (2009) 180–192.

特集：難治性ネフローゼ症候群

# 糖尿病性腎症

和田隆志

日本腎臓学会誌　第52巻 第7号　別刷
（平成22年10月25日発行）

日腎会誌 2010；52(7)：908-913.

特集：難治性ネフローゼ症候群

# 糖尿病性腎症

和田隆志

## はじめに

糖尿病性腎症が新規透析導入の原因疾患の第 1 位になって久しい。2010 年 6 月に日本透析医学会から公表された新規の透析導入患者数は 37,543 名と前年度より 128 名(0.3 %)減少した。一方，糖尿病性腎症による透析導入患者数は 16,414 名と前年度の 16,126 名より増加している。この背景には，糖尿病患者数自体の増加も影響している[1]。さらに，2 型糖尿病患者は 1 型糖尿病患者と比較して医療機関受診率が低いことも以前より指摘されている。さらに，CKD ステージ 3 以降の糖尿病性腎症の予後をみると，尿蛋白量が多いほどその予後が不良であることが示されている[2]。これらの点から，2 型糖尿病の顕性蛋白尿例，特にネフローゼ症候群を生じている糖尿病性腎症例は腎予後が不良な難治例であるため，糖尿病性腎症の発症を未然に防ぐ方策とともに，集約的治療，予後改善が臨床的な重要課題である。

そこで本稿では，糖尿病性腎症，特にネフローゼ症候群を生じる進行性の病態について，疫学，臨床的特徴，治療を中心に概説する。

## 糖尿病性腎症の疫学：腎臓病総合レジストリーの有用性

これまで，本邦における公的機関による糖尿病性腎症登録とそれに基づく医療統計の基盤，疫学的評価の基盤は十分に整備されていなかった。しかし近年，日本腎臓学会が推進している腎臓病総合レジストリーの解析により，本邦における糖尿病性腎症の頻度ならびにその臨床病理学的な特徴が浮き彫りになってきた[3]。2009 年末までに腎臓病総合レジストリーに 6,476 例が登録され，このうち糖尿病性腎症関連登録例として組織診断確定，代謝性疾患に伴う腎障害あるいは CRF/CKD 登録の糖尿病診断有りと DM 登録から，458 例(J-RBR 334 例，J-KDR 109 例，CRF/CKD 登録 5 例，DM 登録 10 例；男性 325 例，女性 133 例；年齢 14〜91 歳，平均 60.5 歳)が抽出された。このうち，糖尿病性腎症の組織学的確定例(281 例)における臨床診断は，代謝性疾患に伴う腎障害 108 例(38.4 %)，ネフローゼ症候群 75 例(26.7 %)，ネフローゼ症候群＋代謝性疾患に伴う腎障害 36 例(12.8 %)，慢性腎炎症候群 41 例(14.6 %)とその 39.5 %がネフローゼ状態を伴う進行例であることが明らかとなった(**図 1**)。これを反映して検尿所見では，尿蛋白定性 1＋以上が 90 %以上，平均 4.3 g/日の高度蛋白尿に加えて，尿潜血陽性を 49.5 %に認めた[3]。

一方，早期の糖尿病性腎症を含めた疫学，病態の理解，

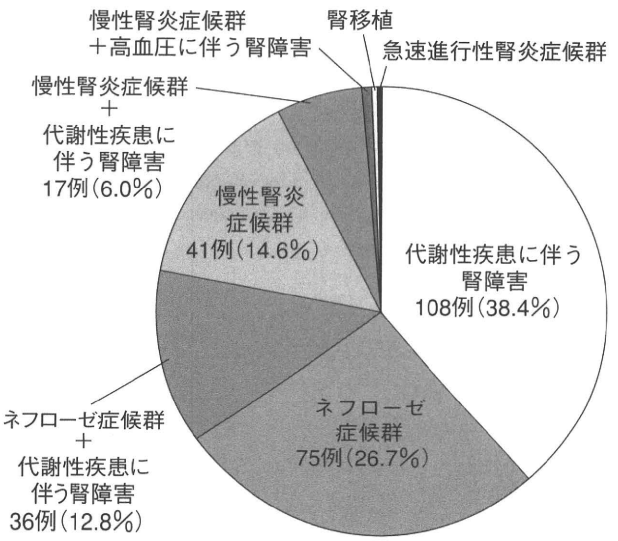


**図 1　腎臓病総合レジストリー：糖尿病性腎症の組織診断確定例の臨床診断（n＝281）**

*Diabetic nephropathy and nephrotic syndrome*
金沢大学医薬保健研究域医学系血液情報統御学
同 附属病院腎臓内科

**表 1 糖尿病性腎症病期分類**

| 病期 | 臨床的特徴<br>蛋白尿(アルブミン) | GFR(Ccr) | 病理学的特徴<br>(糸球体病変) | 備考<br>(主な治療法) |
|---|---|---|---|---|
| 第 1 期<br>(腎症前期) | 正常 | 正常<br>ときに高値 | びまん性病変：<br>ない～軽度 | 血糖コントロール |
| 第 2 期<br>(早期腎症) | 微量アルブミン尿 | 正常<br>ときに高値 | びまん性病変：<br>軽度～中等度<br>結節性病変：<br>ときに存在 | 厳格な血糖コントロール・降圧療法 |
| 第 3 期 A<br>(顕性腎症前期) | 持続的蛋白尿 | ほぼ正常 | びまん性病変：<br>中等度<br>結節性病変：<br>多くは存在 | 厳格な血糖コントロール・降圧療法<br>・蛋白制限食 |
| 第 3 期 B<br>(顕性腎症後期) | 持続的蛋白尿 | 低下 | びまん性病変：<br>高度<br>結節性病変：<br>多くは存在 | 厳格な降圧療法・<br>蛋白制限食 |
| 第 4 期<br>(腎不全期) | 持続的蛋白尿 | 著明低下<br>(血清クレアチニン値上昇) | 荒廃糸球体 | 厳格な降圧療法・<br>蛋白制限食<br>透析療法導入 |
| 第 5 期<br>(透析療法) | 透析療法中 | | | 移植 |

治療への展望をするうえで，糖尿病専門医から成る糖尿病データマネジメント研究会(JDDM)からの報告が参考になる[4]。現在，早期の糖尿病性腎症は臨床的に微量アルブミン尿の出現した時点で診断される[5]。この早期腎症は全体の 32 %で腎症の 76 %を占めている。次に糖尿病性腎症の病期分類を**表 1** に示す[6]。病理学的には，糖尿病性腎症の早期にはびまん性病変が軽度にみられ，その病期の進行とともにびまん性病変の進展，結節性病変がみられるようになる。このうちネフローゼ症候群は第 3 期 B から第 4 期にわたってみられる。第 3 期である顕性腎症期は 7 %，第 4 期の腎不全期は 2.6 %，第 5 期の透析療法期は 0.4 %と早期腎症と併せ計 42 %に腎症がみられるとされるが，このうちどの程度がネフローゼ症候群を示すかは不明である。一方微量アルブミン尿による診断では，2006 年に報告された DEMAND Study において 39 %，アジア人を対象とした MAP Study では 40 %が腎症とされ，アジア人はコーカシアンに比べて微量アルブミン尿，顕性蛋白尿の頻度が高いことが示されている。

現在，腎臓病総合レジストリーを用いて，腎生検の有無にかかわらず，糖尿病性腎症の臨床所見の経年的な統計調査を行うことが可能となった。このことは，本邦における糖尿病性腎症の診療実態調査，病態把握，予後改善や有効な治療法開発に向けた総合的なシステム構築につながる可能性がある。さらに，この腎臓病総合レジストリーの二次研究として，糖尿病性腎症レジストリー(JDN-CS)が構築され，平成 21 年度より運用されている。非腎生検例も含め，早期腎症から進行した腎症まで糖尿病性腎症の病態把握，予後調査を含めた総合的な実態調査の基盤が整備され，今後のシステムの充実とその有効な活用が期待される。

## ネフローゼ症候群における糖尿病性腎症

腎臓病総合レジストリーにおいて，臨床分類のネフローゼ症候群 1,197 例に占める糖尿病性腎症の割合は 10.7 %であった(**図 2a**)[3]。これは，原発性(一次性)糸球体疾患の 61.0 %(IgA 腎症を含むと 66.2 %)に次ぐ頻度であった。さらに，1961 年より当科にて腎生検にて病理診断を行ったネフローゼ症候群 721 例の経時的な推移を確認したところ，糖尿病性腎症によるネフローゼ症候群の増加が顕著であった(図 2b)。ただし糖尿病性腎症によるネフローゼ症候群は腎生検を施行していない例もあることから，過小評価している可能性がある。また臨床的には，ネフローゼ症候群の成因や経過を考えるうえで，他の腎臓病の合併，主病因によるネフローゼ症候群の経過中に糖尿病がもたらす影響も

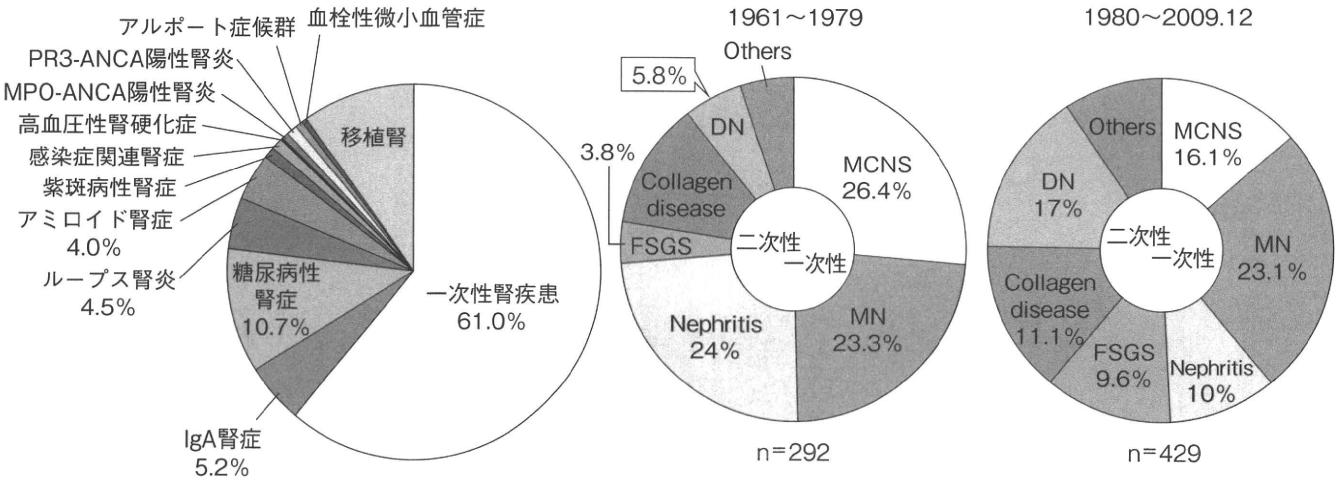


a．ネフローゼ症候群(1,197 例)における病理病因分類　　b．ネフローゼ症候群に占める糖尿病性腎症の割合は増加している。

**図 2　ネフローゼ症候群に占める糖尿病性腎症の頻度**

MCNS：微小変化型ネフローゼ症候群，MN：膜性腎症，Nephritis：腎炎，FSGS：巣状分節性糸球体硬化症，Collagen disease：膠原病，DN：糖尿病性腎症

考える必要がある。加えて，年齢層別に比較して検討すると，いずれの年齢層別でも一次性糸球体疾患が主体であったが，40 歳以降に糖尿病性腎症の占める割合が増加していた[3]。

## 糖尿病性腎症病期分類と CKD のステージ(病期)分類

前述したように，現在用いられている糖尿病性腎症病期分類は，主として尿アルブミン/尿蛋白を用いて病期分類がなされている(表 1)。一方，CKD のステージ分類は腎機能の評価指標である糸球体濾過量(GFR)を主体としている[7]。したがって，糖尿病性腎症のうち両者が乖離する例，すなわち尿アルブミン/尿蛋白がみられない腎機能低下例，あるいは腎機能の保たれた顕性腎症例(ネフローゼ症候群例)が存在する。このような症例の臨床症状を裏づける病理学的な評価はいまだ十分ではない。こういった乖離例の病態，末期腎不全に至る腎予後とその因子，心血管病変の発症・進展様式，生命予後などの評価は今後の重要な臨床的検討項目と考えられる。このように，CKD のステージ分類と糖尿病性腎症病期分類との整合性も改めて課題となっている。

## 糖尿病性腎症とバイオマーカー

糖尿病性腎症の早期診断は予後の改善のために重要である。現在，早期糖尿病性腎症の診断に用いられる微量アルブミン尿は，特異性，日内変動，腎機能低下との相関性など臨床的な問題点も有する。実際，微量アルブミン尿は腎症の診断や病態把握に用いられる一方，心血管事故の危険因子であることも知られている[8]。さらに，微量アルブミン尿陰性例においても腎機能低下を示す，あるいは進行性の糖尿病性病変を有する例が存在することが知られている。したがって，他の腎臓病を鑑別すべく，より特異性が高い，かつより早期から診断可能なバイオマーカーの開発と，その臨床応用は喫緊の課題である。これまでに糖尿病性腎症の特徴であり，腎機能と相関するメサンギウム拡大と関連が深い尿 Smad 1 の有用性が示されている[9]。しかしながら，ヒト糖尿病性腎症において，より有用かつ特異的な早期診断マーカーはいまだない。今後，早期診断のみならず，ネフローゼ症候群を呈する進行例を含めて，治療効果判定，予後判定に有用な新たなバイオマーカーの開発が期待される。

## 糖尿病性腎症の病理所見

糖尿病性腎症，特に糸球体の病理所見として，メサンギウム基質の増加・蓄積を示す硬化性病変と糖蛋白や脂肪を含む血漿成分の貯留をみる滲出性病変がある[10]。糖尿病性腎症の組織学的な表現型として，糸球体病変以外に動脈および細動脈の硝子化，血管病変に基づくとされる間質病変，尿細管基底膜の肥厚，ならびに尿細管上皮の空胞変性など

が知られている[10]。糸球体病変のうち，硬化性病変は糸球体硬化症と呼ばれ，結節性硬化とびまん性硬化の2つに大別される。このうち，結節性病変は最も特徴的で診断価値が高く，臨床的にはネフローゼ症候群を呈する進行性の病態を反映している。この典型的な糖尿病性腎症の所見を1936年にKimmelstiel，Wilsonが報告し，Kimmelstiel-Wilson結節とも呼ばれている[11]。この進展様式として，びまん性病変が係蹄末梢部で進展することによって生じ，主として，①IV型コラーゲンの蓄積がみられる病変，②メサンギウム融解現象との関連も示唆されているPAM淡染性のVI型コラーゲンの蓄積を特徴とする病変，が報告されている[12]。その病態形成の詳細な機序は目下のところ不明であるが，megsin，iNOS，RAGEのトリプルトランスジェニックマウスにおいて，30〜40％の糸球体に結節性病変様の所見がみられると報告され興味深い[13]。また，濾過面をもたない血管を中心に基質が年輪状に蓄積して結節が構成され，その様相から“doughnut lesion”と呼ばれる病変は，糖尿病性腎症以外ではほとんど認められない特徴的な所見である[14]。一方，血管病変においても，輸入細動脈に加えて輸出細動脈の硝子化は糖尿病性腎症以外の疾患で認めることはほとんどなく，特異性が高い病変の一つである[10]。

## 糖尿病性腎症の治療

現在，糖尿病性腎症の治療は**表2**に示すごとく集約的治療が提示されている[15]。このうち，生活習慣の改善に加えて，1）高血糖の長期間の厳密なコントロール，2）全身血圧の厳格なコントロールならびに糸球体高血圧の是正，が基本となる。

血糖コントロールにより糖尿病性腎症に代表される細小血管病変の進展が抑制されることは，1型糖尿病を対象としたDCCT試験[16,17]，2型糖尿病を対象としたKumamoto study[18]，UKPDS試験[19]，ならびにThe ADVANCE Collaborative Groupの研究[20]といった大規模臨床試験でも示されている。このうち，UKPDS試験では$HbA_{1c}$ 1％低下することにより細小血管障害合併の危険率が37％減少することも示されている。「エビデンスに基づくCKD診療ガイドライン2009」では，治療目標を$HbA_{1c}$ 6.5％未満としている。なお，2010年7月に新しい糖尿病診断基準が発表され，$HbA_{1c}$のカットオフ値はJDS値で6.1％，NGSP相当値で6.5％とされている。

さらに血圧コントロールは治療上の重要な要素である。このうち，「エビデンスに基づくCKD診療ガイドライン2009」では高血圧を合併した糖尿病例の降圧目標は130/80 mmHg未満としている。さらに，尿蛋白が1 g/日以上では平均血圧92 mmHg未満（125/75 mmHgに相当）を目標とすることが明記されている。しかしながら，降圧目標達成率が低いことも示されている[21]。第一選択薬はアンジオテンシン変換酵素阻害薬（ACEI），アンジオテンシンII受容体拮抗薬（ARB）と記されている。これにより，全身血圧の厳格なコントロールとともに，糸球体の輸出細動脈の拡張から糸球体高血圧の是正をきたすことが期待されている。実際，本邦においてもJAPAN-IDDMにおいて，早期ならびに顕性腎症期におけるACEIの腎保護作用が示された[22]。一方，2型糖尿病において，微量アルブミン尿を呈する正常腎機能例におけるACEIによる腎保護作用が示されている[23]。特に，糖尿病性腎症によるネフローゼ症候群に対して，ACEIを投与したところ，2週間以内に平均10.6 g/日から6.1 g/日へと尿蛋白が減少したことをTagumaらが先駆けて報告している[24]。さらにKasiskeらは1，2型糖尿病を対象として施行された100臨床試験についてメタアナリシスを行った。その結果，全身の降圧とは無関係に，他の降圧薬とは異なるACEIの蛋白尿減少効果ならびに腎機能保持効果を示した[25]。一方，ARBを用いた大規模臨床試験では2型糖尿病の微量アルブミン例[26,27]，顕性蛋白尿例[28]に対する有効性が報告されている。加えて，ARBに直接的レニン阻害薬を追加投与することで，高血圧合併2型糖尿病性腎症例における蛋白尿（アルブミン尿）の減少効果が報告されている[29]。

最近になり，糖尿病性腎症の治療は寛解（remission）と退縮（regression）を目指す治療へと変化してきている。これは，単独膵移植を行った後，1型糖尿病例の腎組織を長期経過観察した研究結果が発端となった。すなわち，膵臓移植による血糖正常化後10年で，当初みられた腎症が改善

**表2　糖尿病性腎症の集約的治療**

| | |
|---|---|
| 1 | 生活習慣の改善<br>減量，運動，蛋白質・食塩・アルコール制限，禁煙 |
| 2 | 高血糖の是正：厳格な血糖コントロール（$HbA_{1c}$値＜6.5％） |
| 3 | 糸球体高血圧の是正：<br>・レニン・アンジオテンシン系阻害薬〔アンジオテンシン変換酵素阻害薬（ACEI），アンジオテンシンII受容体拮抗薬（ARB）〕の使用<br>・全身血圧の管理：目標血圧値＜130/80 mmHg<br>（長時間作用型Ca拮抗薬，利尿薬を併用） |
| 4 | 血清脂質の管理（スタチン） |
| 5 | 蛋白質制限食（0.8 g/kg/日） |

し寛解(remission)と退縮(regression)が起こることが示されたことによる。本邦においても，2型糖尿病の早期腎症例に対して寛解(remission)が期待される知見が得られている[30]。特に，寛解(remission)に関与する因子として，1）微量アルブミン尿の出現期間が短いこと，2）レニン・アンジオテンシン系（RAS)阻害薬を使用していること，3）血糖コントロールが良好なこと，4）収縮期血圧が低いことが重要とされている。さらに，2年間経過観察を延長したところ，アルブミン尿の寛解もしくは50％以上の減少を認めた例では，腎機能低下速度の抑制，心血管病変抑制がみられたことは注目される[31]。

## まとめ

糖尿病性腎症，特にネフローゼ症候群を示す進行例の疫学，臨床的特徴，治療を中心に概説した。糖尿病性腎症の予後を改善するうえで予防に勝る治療法はない。発症予防から一連の治療において，日常生活全般に密接にかかわる食事療法ならびに包括的に支援するチーム医療の役割は薬物治療と並んで今後ますます重要視されることと推測される。糖尿病性腎症の発症予防，予後改善に向けて，実態把握，早期診断，病態解明，治療法確立といった総合的な取り組みが一層期待される。

## 文　献


1. 厚生労働省健康局総務課生活習慣病対策室．平成19年国民健康・栄養調査の概要．
2. Rigalleau V, Lasseur C, Raffaitin C, Beauvieux MC, Barthe N, Chauveau P, Combe C, Gin H. Normoalbuminuric renal-insufficient diabetic patients：a lower-risk group. Diabetes Care 2007；30：2034-2039.
3. 横山　仁．厚生労働科学研究費補助金　腎疾患対策研究事業　糖尿病性腎症の病態解明と新規治療法確立のための評価法の開発(研究代表者　和田隆志)．平成21年度総括・分担研究報告書，21-27.
4. Yokoyama H, Kawai K, Kobayashi M；Japan Diabetes Clinical Data Management Study Group. Microalbuminuria is common in Japanese type 2 diabetic patients：a nationwide survey from the Japan Diabetes Clinical Data Management Study Group(JDDM 10). Diabetes Care 2007；30：989-992.
5. 猪俣茂樹，羽田勝計，守屋達美，他．糖尿病性腎症の新しい早期診断基準．糖尿病 2005；48：757-759.
6. 糖尿病性腎症に関する合同委員会．糖尿病性腎症病期分類厚生省案の改定について．糖尿病 2001；44：623.
7. 日本腎臓学会編．CKD診療ガイド．東京：東京医学社，2009：12-13.
8. Adler AI, Stevens RJ, Manley SE, Bilous RW, Cull CA, Holman RR；UKPDS GROUP. Development and progression of nephropathy in type 2 diabetes：the United Kingdom Prospective Diabetes Study(UKPDS 64). Kidney Int 2003；63：225-232.
9. Mima A, Arai H, Matsubara T, Abe H, Nagai K, Tamura Y, Torikoshi K, Arai M, Kanamori H, Takahashi T, Tominaga T, Matsuura M, Iehara N, Fukatsu A, Kita T, Doi T. Urinary Smad 1 is a novel marker to predict later onset of mesangial matrix expansion in diabetic nephropathy. Diabetes 2008；57：1712-1722.
10. 北村博司．糖尿病性腎症の組織分類　腎生検病理診断標準化への指針．日本腎臓学会・腎病理診断標準化委員会(編)．2005：167-174.
11. Kimmelstiel P, Wilson C. Intercapillary lesions in the glomeruli of the kidney. Am J Pathol 1936；12：83-98.7.
12. Saito Y, Kida H, Takeda S, Yoshimura M, Yokoyama H, Koshino Y, Hattori N. Mesangiolysis in diabetic glomeruli：its role in the formation of nodular lesions. Kidney Int 1988；34：389-396.
13. Inagi R, Yamamoto Y, Nangaku M, Usuda N, Okamato H, Kurokawa K, van Ypersele de Strihou C, Yamamoto H, Miyata T. A severe diabetic nephropathy model with early development of nodule-like lesions induced by megsin overexpression in RAGE/iNOS transgenic mice. Diabetes 2006；55：356-366.
14. Yajima G. A histopathological study on diabetic nephropathy-light and electron microscopic observations. Acta Pathol Jpn 1976；26：47-62.
15. 羽田勝計．糖尿病性腎症　初学者から専門医までで腎臓学入門　改定第2版．日本腎臓学会編集委員会(編)．東京：東京医学社，2009：129-137.
16. Diabetes control and complications trial research group. The effect of intensive treatment of diabetes on the development and progression of long-term complications in insulin-dependent dibetes mellitus. N Engl J Med 1993；329：977-986.
17. The diabetes control and complication trial/epidermiology of diabetes interventions and complications research group. Retinopathy and nephropathy in patients with type 1 diabetes four years after trial of intensive therapy. N Engl J Med 2000；342：381-389.
18. Ohkubo Y, Kishikawa H, Araki E, et al. Intensive insulin therapy prevents the progression of diabetic microvascular complications in Japanese patients with non-insulin-dependent diabetes mellitus：a randomized prospective 6-year study. Diabetes Res Clin Pract 1995；28：103-117.
19. UK Prospective Diabetes Study Group. Intensitve blood glucose control with sulphonylureas or insulin compared with conventional treatment and risk of complications in patients with type 2 diabetes(UKPDS 33). Lancet 1998；352：837-853.
20. ADVANCE Collaborative Group. Intensive blood glucose control and vascular outcomes in patients with type 2 diabetes. N Engl J Med 2008；358：2560-2572.

21. 藤田敏郎, 寺本民生. 高血圧および高脂血症の薬物療法の現状と課題 Japan Guideline Assessment Panel (J-GAP). Progress in Medicine 2006 ; 26 : 2297-2306.
22. Katayama S, Kikkawa R, Isogai S, Sasaki N, Matsuura N, Tajima N, Urakami T, Uchigata Y, Ohashi Y. Effect of captopril or imidapril on the progression of diabetic nephropathy in Japanese with type 1 diabetes mellitus : a randomized controlled study (JAPAN-IDDM). Diabetes Res Clin Pract 2002 ; 55 : 113-121.
23. Ravid M, Lang R, Rachmani R, Lishner M. Long-term renoprotective effect of angiotensin-converting enzyme inhibition in non-insulin-dependent diabetes mellitus. A 7-year follow-up study. Arch Intern Med 1996 ; 156 : 286-289.
24. Taguma Y, Kitamoto Y, Futaki G, Ueda H, Monma H, Ishizaki M, Takahashi H, Sekino H, Sasaki Y. Effect of captopril on heavy proteinuria in azotemic diabetics. N Engl J Med 1985 ; 313 : 1617-1620.
25. Kasiske BL, Kalil RS, Ma JZ, Liao M, Keane WF. Effect of antihypertensive therapy on the kidney in patients with diabetes : a meta-regression analysis. Ann Intern Med 1993 ; 118 : 129-138.
26. Parving HH, Lehnert H, Bröchner-Mortensen J, Gomis R, Andersen S, Arner P ; Irbesartan in Patients with Type 2 Diabetes and Microalbuminuria Study Group. The effect of irbesartan on the development of diabetic nephropathy in patients with type 2 diabetes. N Engl J Med 2001 ; 345 : 870-878.
27. Makino H, Haneda M, Babazono T, Moriya T, Ito S, Iwamoto Y, Kawamori R, Takeuchi M, Katayama S ; INNOVATION Study Group. Prevention of transition from incipient to overt nephropathy with telmisartan in patients with type 2 diabetes. Diabetes Care 2007 ; 30 : 1577-1578.
28. Brenner BM, Cooper ME, de Zeeuw D, Keane WF, Mitch WE, Parving HH, Remuzzi G, Snapinn SM, Zhang Z, Shahinfar S ; RENAAL Study Investigators. Effects of losartan on renal and cardiovascular outocomes in patients with type 2 diabetes and nephropathy. N Engl J Med 2001 ; 345 : 861-869.
29. Parving HH, Persson F, Lewis JB, Lewis EJ, Hollenberg NK ; AVOID Study Investigators. Aliskiren combined with losartan in type 2 diabetes and nephropathy. N Engl J Med 2008 ; 358 : 2433-2446.
30. Araki S, Haneda M, Sugimoto T, Isono M, Isshiki K, Kashiwagi A, Koya D. Factors associated with frequent remission of microalbuminuria in patients with type 2 diabetes. Diabetes 2005 ; 54 : 2983-2987.
31. Araki S, Haneda M, Koya D, Hidaka H, Sugimoto T, Isono M, Isshiki K, Chin-Kanasaki M, Uzu T, Kashiwagi A. Reduction in microalbuminuria as an integrated indicator for renal and cardiovascular risk reduction in patients with type 2 diabetes. Diabetes 2007 ; 56 : 1727-1730.

Human Pathology (2010) 41, 672–678

ELSEVIER

Human PATHOLOGY

www.elsevier.com/locate/humpath

Original contribution

# Fibrocytes are involved in the pathogenesis of human chronic kidney disease☆

**Norihiko Sakai MD, PhD[a], Kengo Furuichi MD, PhD[a], Yasuyuki Shinozaki MD[b], Hiroyuki Yamauchi MD[b], Tadashi Toyama MD[b], Shinji Kitajima MD[b], Toshiya Okumura MD[b], Satoshi Kokubo MD[b], Motoo Kobayashi MD[b], Kazuya Takasawa MD, PhD[d], Shin-ichi Takeda MD, PhD[e], Mitsuhiro Yoshimura MD, PhD[f], Shuichi Kaneko MD, PhD[b], Takashi Wada MD, PhD[c,*]**

[a]*Division of Blood Purification, Kanazawa University Hospital, Kanazawa 920-8641, Japan*
[b]*Faculty of Medicine, Department of Disease Control and Homeostasis, Institute of Medical, Pharmaceutical and Health Sciences, Kanazawa University, Kanazawa 920-8641, Japan*
[c]*Faculty of Medicine, Department of Laboratory Medicine, Institute of Medical, Pharmaceutical and Health Sciences, Kanazawa University, Kanazawa 920-8641, Japan*
[d]*Department of Internal Medicine, Public Central Hospital of Matto Ishikawa, Hakusan 924-8588, Japan*
[e]*Department of Internal Medicine, Kurobe Municipal Hospital, Kurobe 933-8502, Japan*
[f]*Department of Internal Medicine, Kanazawa Medical Center, Kanazawa 920-8650, Japan*

Received 5 August 2009; revised 30 September 2009; accepted 8 October 2009

**Keywords:**
CKD;
Fibrocytes;
Fibrosis;
Chemokine

**Summary** The presence of chronic kidney disease in humans is associated with a risk of kidney function loss as well as the development of cardiovascular disease. Fibrocytes have been shown to contribute to organ fibrosis. In this study, the presence of fibrocytes was investigated immunohistochemically in kidney biopsy specimens from 100 patients with chronic kidney disease. In addition, 6 patients with thin basement membrane disease were studied as a disease control. In patients with chronic kidney disease, the infiltration of fibrocytes was observed mainly in the interstitium. The number of interstitial fibrocytes in patients with chronic kidney disease was higher than that in patients with thin basement membrane disease. The number of infiltrated fibrocytes in the interstitium correlated well with the severity of tubulointerstitial lesions, such as interstitial fibrosis, in patients with chronic kidney disease. In addition, there were significant correlations between the number of interstitial fibrocytes and the number of CD68-positive macrophages in the interstitium as well as urinary monocyte chemoattractant protein-1/CCL2 levels. In particular, there was an inverse correlation between the number of interstitial fibrocytes and kidney function at the time of biopsy. Finally, the numbers of interstitial fibrocytes and macrophages as well as urinary CCL2 levels were significantly decreased during convalescence induced by glucocorticoid therapy. These results suggest that fibrocytes may be involved in the pathogenesis of chronic kidney disease through the interaction with macrophages as well as CCL2.


☆ This work was supported by a Grant-in-aid from the Ministry of Education, Science, Sport and Culture of Japan and Takeda Science Foundation (T.W.) and CKD AWARD 2008 from Nippon Boehringer Ingelheim Co, Ltd, and Astellas Pharma Inc (NS).
* Corresponding author.
*E-mail address:* twada@m-kanazawa.jp (T. Wada).

0046-8177/$ – see front matter © 2010 Elsevier Inc. All rights reserved.
doi:10.1016/j.humpath.2009.10.008

## 1. Introduction

The presence of chronic kidney disease (CKD), manifested by low glomerular filtration rates (GFR) and/or urinary abnormalities, is associated with risk of kidney function loss leading to end-stage renal disease (ESRD). Recently, CKD has also been recognized as an independent risk factor of cardiovascular disease [1]. Therefore, it is important to elucidate the pathophysiology of CKD. Despite varied etiologies, CKD progresses to ESRD through common pathological findings, including glomerulosclerosis and interstitial fibrosis. Especially, the severity of interstitial fibrosis has been reported to determine the prognosis of kidney function [2]. To date, resident fibroblasts, epithelial-mesenchymal transition (EMT)–derived fibroblasts/myofibroblasts, and monocytes/macrophages have been suggested to be involved in the progression of kidney diseases [3,4]. However, the precise pathogenic mechanisms of tubulointerstitial lesions, especially related to interstitial fibrosis, in patients with CKD remain to be determined.

Recently, a circulating bone marrow-derived population of fibroblast-like cells, termed fibrocytes, has been proposed to be a new cellular participant in the pathogenesis of organ fibrosis [5-9]. Fibrocytes express markers of leukocytes (eg, CD45 and CD34) and have the ability to produce extracellular matrix proteins (eg, type I collagen and fibronectin) [10,11]. The presence of fibrocytes has been demonstrated in experimental fibrosis associated with various conditions, such as lung, kidney, and liver fibrosis, as well as skin wounds [5-9]. Fibrocytes are also detected in human fibrosing disorders, including nephrogenic systemic fibrosis, bronchial asthma, and burns [12-14]. Fibrocytes have been reported to express chemokine receptors such as CCR2, CCR7, and CXCR4 [5,6,15,16]. In addition, fibrocytes are capable of producing various chemokines including monocyte chemoattractant protein–1/CCL2 as well as fibrogenic cytokines (eg, transforming growth factor [TGF]–$\beta$1) [10]. Recent studies demonstrated that chemokine/chemokine receptor systems are required for the recruitment of fibrocytes to sites of fibrosis [5,6,8,16]. However, the involvement of fibrocytes in the pathogenesis of human CKD has not been fully investigated.

From these findings, we hypothesized that fibrocytes dependent on chemokine/chemokine receptor systems are involved in the pathogenesis of human CKD. To achieve this goal, we determined the presence of fibrocytes in patients with CKD. We also examined the association of fibrocytes infiltration with pathological findings as well as urinary levels of chemokines.

## 2. Subjects and methods

### 2.1. Subjects

One hundred patients (41 men and 59 women; median age, 50.2 years) with CKD were evaluated in this study (Table 1). CKD was defined as urinary abnormalities or GFR <60 mL/min per 1.73 $m^2$ for 3 months or more irrespective of cause, as described previously [17]. Twenty-seven patients (10 men and 17 women; median age, 62.5 years) had crescentic glomerulonephritis (CreGN) with more than 50% of the total crescents (cellular, fibrocellular, and fibrous) of all glomeruli showing rapidly progressive glomerulonephritis clinically. Twenty-six patients (2 men and 24 women; median age, 37.2 years) had lupus nephritis (LN) and were classified based on the glomerular appearance according to the International Society of Nephrology/Renal Pathology Society 2003 classification (8 in class II, 5 in class III, 9 in class IV, 4 in class V) as described previously [18]. Twenty-three patients with type 2 diabetes mellitus (14 men and 9 women; median age, 55.8 years) had diabetic nephropathy (DN). In addition, other kidney diseases without crescents, including IgA nephropathy (IgA-N), obesity-related glomerulopathy (ORG), benign nephrosclerosis (BNS), and membranous nephropathy (MN), were also examined in this study. Six patients with thin basement membrane disease (TBMD; 4 men and 2 women; median age, 39.1 years) were included as disease controls. The patients in this study were chosen consecutively from May 1988 to July 2008 at Kanazawa University Hospital or its affiliated hospitals. All diagnoses were verified by kidney biopsy. Whenever possible, patients did not receive immunosuppressive agents before sample collection. Patients with CreGN, LN, or IgA-N in a clinically active state were treated with glucocorticoids including methylprednisolone pulse therapy (500-1000 mg/day, 3 days) during this study. Specimens from second biopsies were obtained from 16 patients with CreGN ($n$ = 7), LN (n = 7), and IgA-N (n = 2) after glucocorticoid therapy. Estimated glomerular filtration rate (eGFR) was determined as reported previously [19]. All kidney biopsies and this study were performed with approval from the Institutional Review Board and on receipt of informed consent from the patients.

### 2.2. Pathologic studies

One hundred twenty-two kidney specimens were obtained by kidney biopsy. Each specimen contained 10 or more

**Table 1** Patient Profiles

| Diagnosis | No. of patients (men:women) | Mean age (year) | Fibrocytes/field (×200) |
|---|---|---|---|
| CreGN | 27(10:17) | 62.5 | 13.3 ± 1.8 [a] |
| LN | 26(2:24) | 37.2 | 6.8 ± 1.4 [a, b] |
| DN | 23(14:9) | 55.8 | 7.6 ± 0.9 [a, b] |
| IgA-N | 8(4:4) | 28.3 | 3.9 ± 0.9 [a, b] |
| ORG | 8(5:3) | 45.4 | 3.6 ± 1.2 [b] |
| MN | 4(4:0) | 54.1 | 3.7 ± 1.6 [b] |
| BNS | 4(2:2) | 63.8 | 4.6 ± 1.1 [a, b] |
| TBMD | 6(4:2) | 39.1 | 0.9 ± 0.4 [b] |

Values are mean + SE.
[a] $P < .05$ versus thin basement membrane disease.
[b] $P < .05$ versus crescentic glomerulonephritis.

glomeruli. Kidney specimens were fixed in 10% buffered formalin (pH 7.2), embedded in paraffin, cut into sections 4 μm thick and stained with hematoxylin and eosin, periodic acid–Schiff reagent, periodic acid silver methenamine, and Mallory-Azan. Two observers with no knowledge of the patients' clinical course examined the kidney specimens by light microscopy to establish the diagnosis. For patients with CreGN, the percentages of crescent formation were evaluated. For DN patients, the severity of the diffuse lesions of glomeruli was graded on a scale of 0 to IV, as described previously [20]. For LN patients, International Society of Nephrology/Renal Pathology Society 2003 classification was used for light microscopic classification of LN. For all patients, the mean interstitial fibrotic area (blue on Mallory-Azan staining) was determined and expressed as percentage per square millimeter of the field using Mac Scope version 6.02 (Mitani Shoji Co, Ltd, Fukui, Japan). Similarly, for evaluation of glomerulosclerosis, mean mesangial area (black on periodic acid silver methenamine staining) per glomerulus was examined from more than 10 glomeruli using Mac Scope version 6.02 (Mitani Shoji Co, Ltd) as reported previously [20].

### 2.3. Immunohistochemical studies

Fibrocytes were identified by dual immunohistochemical techniques on formalin-fixed, paraffin-embedded tissue specimens using specific antibodies against CD45 and type I pro-collagen α1 (proCOLI), as described previously [13]. Briefly, CD45 was detected by the indirect avidin-biotinylated alkaline phosphatase method using a murine anti-human CD45 monoclonal antibody (DAKO, Glostrup, Denmark). Type I proCOLI (Santa Cruz Biotechnology, Inc, Santa Cruz, CA) was detected using the indirect avidin-biotinylated peroxidase complex method. In this dual immunostaining, the color of CD45-positive cells was red, while type I proCOLI-positive cells were brown. CD68-positive macrophages were also detected immunohistochemically on formalin-fixed, paraffin-embedded tissue sections by the indirect avidin-biotinylated alkaline phosphatase complex method using a murine anti-human macrophage CD68 monoclonal antibody (clone KP1; DAKO). As a positive control, resected tonsils from patients with tonsillitis were used. Mean numbers of interstitial CD45/type I proCOLI dual-positive fibrocytes as well as CD68-positive macrophages were counted from more than 10 randomly chosen fields under high-power magnification (200×). Two independent observers also examined the immunohistochemical findings without prior knowledge of chemokine levels or the patients' clinical courses.

### 2.4. Measurements of urinary chemokines

Spontaneously voided midstream urine catches were collected on the morning of kidney biopsy. Samples of 10 mL of the each urine specimen were spun at 200*g* for 5 minutes at room temperature to remove cells and precipitate. The urinary supernatants were kept frozen at −70°C until measurement. Urinary CCL2 levels were determined by enzyme-linked immunosorbent assay (ELISA), using a specific murine monoclonal anti-human CCL2 antibody (clone ME69) for capture and a rabbit anti-CCL2 polyclonal antibody as the second antibody, as described previously [21]. The recovery rate was confirmed to be more than 95% up to 3 ng/mL in these ELISA systems. The urinary levels of stromal cell-derived factor-1α/CXCL12, a ligand for CXCR4, as well as secondary lymphoid tissue chemokine/CCL21, a ligand for CCR7, were also determined using ELISA kits (R&D Systems, Minneapolis, MN). All assays were performed in duplicate. The detection limits of this ELISA system were 40 pg/mL for CCL2, 18 pg/mL for CXCL12, and 9.9 pg/mL for CCL21. Urinary levels of these chemokines were standardized by the amount of creatinine in the urine. All kidney biopsies were performed with the informed consent of the patients. Urinary tract infections were excluded in all cases by bacterial culture, microscopic findings, or both, because urinary tract infection is associated with increased urinary CCL2 levels (data not shown).

### 2.5. Statistics

Statistical significance was analyzed using paired or unpaired Student *t* test, analysis of variance, and Spearman and Pearson correlation coefficients for analyses of non-parametric and parametric data. $P < .05$ was considered to indicate statistical significance.

## 3. Results

### 3.1. Fibrocytes infiltrating the interstitium in patients with CKD

To determine the presence of fibrocytes, kidney samples from 100 patients with CKD, including CreGN, LN, DN, IgA-N, ORG, MN, and BNS, and 6 patients with TBMD were examined by immunohistochemical analyses. In patients with CKD, CD45/proCOLI dual-positive fibrocytes were observed mainly in the interstitium (Fig. 1A). The number of interstitial fibrocytes in patients with CKD was higher than that in patients with TBMD (8.1 ± 0.7 versus 0.9 ± 0.4 per visual field; $P < .01$, Fig. 1B). In contrast, fibrocytes in glomeruli were hardly observed in patients with either CKD or TBMD. The degree of fibrocyte infiltration in patients with CreGN (13.3 ± 1.8 per visual field), LN (6.8 ± 1.4 per visual field), DN (7.6 ± 0.9 per visual field), IgA-N (3.9 ± 0.9 per visual field) as well as BNS (4.6 ± 1.1 per visual field) was more severe than that in TBMD patients (0.9 ± 0.4 per visual field) (Table 1). In addition, the number of interstitial fibrocytes in patients